VOLUME: 4
ISSUE: 1
JUNE 2024

ADVANCED GIS

e-ISSN:2822-7026

Advanced GIS

ADVANCED GIS

e-ISSN: 2687-5179

(VOLUME: 4, ISSUE: 1)

JUNE 2024

Advanced GIS

ABOUT JOURNAL

Advanced GIS (AGIS) journal aims to publish original research articles, review articles and technical notes in the field of Geographic Information Systems (GIS). GIS allows spatial analysis, modeling and visualization of the environment. Nowadays, GIS is actively used in many fields such as agriculture, monitoring of natural disasters, ecology, climate change, polar studies, transportation, defense, education, environment, forest, together with remote sensing. In this context, the AGIS journal focuses on studies in the field of GIS. There is no page limit for the articles to be sent to the AGIS journal.

AIM & SCOPE

Advanced GIS

- To provide an easily accessible and wide-ranging discussion environment that will strengthen and accelerate the sharing of knowledge and experience between scientists, researchers, engineers, and other practitioners who are involved in direct or indirect activities with the following topics.
- To contribute to the initiation and development of inter-institutional cooperation, which is of great importance in terms of solving the problems related to professional developments that can play a role in technological and economic development in the world and Turkey

The scope of Advanced GIS Journal

- GIS, GPS, Remote Sensing and related geospatial studies
- Spatial data infrastructures; standardization and interoperability
- Spatiotemporal analysis
- Spatial Information Management
- 3D modeling and simulation
- Urban Planning Applications
- Disaster Management
- Climate Studies
- Cadastre Applications
- Desktop, mobile and Web-based spatial applications and services

Publication frequency Biannual (June-December)

WEB http://publish.mersin.edu.tr/index.php/agis/index

Contact agis@mersin.edu.tr / mozgurcelik@mersin.edu.tr

Advanced GIS

Contents

Research Articles;

Advanced GIS

http://publish.mersin.edu.tr/index.php/agis/index

e-ISSN:2822-7026

Wildfire hazard and risk assessment: The case of Gabala district

Firuza Aghayeva*[1]

[1]*Institute of Geography named after Akad. Hasan Aliyev, Geoekology, Baku, Azerbaijan*

Keywords
GIS,
Spatial Analysis,
Remote Sensing,
Fire Risk Assessment
DEM

check for updates

Research Article
Received: 04/07/2023
Revised: 17/09/2023
Accepted: 30/11/2023
Published:02/04/2024

Abstract

As one of the main natural resources for humans, protection of forest resources is one of the main ecological problems of the world. Forests are a source of oxygen, as well as they have some features that can ensure ecological balance. For example, forests are one of the major factors that prevent landslides, erosion processes, flood events, as well as protecting land resources, hydrological resources and optimization micro climatic condition. Decreasing of forest stock affects the fauna directly. There are some factors that impact decreasing of forest resources, for example, settlements, industry and forest supply and etcetera. Forest fires occurring in different parts of the world every year eradicated acres of forest stock. The formation of forest fires is influenced by factors such as climate, anthropogenic and topological effects. Research area is district of Gabala, which is situated at south slopes of Greater Caucasus. Gabala is distinguished by the abundance of forest resources in the territory of Azerbaijan, which is poorly provided with forest reserves. 32405.15 hectares of this district are covered with forests. Taking into account that 40% of the fire incidents that occurred on the southern slope of the Greater Caucasus in 2021 and 2022 took place here, this place was taken as a research area. Wildfire hazard and risk assessment and fire risk zonation, anthropogenic and topological effects are considered in this article and mapping had been done. The resulting values were classified according to the risk group and the results were compared with the fire area data. As a result of the comparison, was not found fire process in the categories of no risk or low risk. 90% of fire incidents could be classified as medium risk, high risk and critic high-risk categories. Consequently, this is an indicator of the validity of the selected parameters and the conducted assessment.

1. Introduction

Forest ecosystems, which we can describe as our lungs, are 4 billion hectares covering 1/3 of the world and constitute 75% of biological diversity. Forests have many functions that are extremely vital for the survival of living things, such as maintaining the balance of the climate, protecting soil, water and biological diversity. However, these functions are threatened by factors that put the continuity and sustainability of the forest at risk, such as diseases, insect invasions, drought, unplanned settlements and occupation of the forest by agricultural practices. Among these factors, forest fires are seen as one of the most important damaging factors (Atan et al., 2020; Bar et al., 2020; Kuter et al., 2011). Forest fires affect thousands of hectares each year and cause dramatic changes in forest ecosystems (Başkent, 2018; Başaran et al., 2004; Goldammer & Mutch, 2001;). Approximately 4,000,000 hectares of forest area are damaged in fires in the world every year (Versini, et al., 2013).

One of the most important issues in pre-fire planning is to determine the risk and danger of fire in advance and to take the necessary precautions for sensitive areas. In this respect, the creation of wildfire hazard and risk assessment, fire risk and danger maps is an important base in preventing fire disaster and damage caused by fire (Dong et al., 2006). Generally, forest fire management consists of four steps: mapping fire risk and hazard, monitoring active fires, identifying fire-sensitive areas, and identifying post-fire deterioration (Betanzos et al., , 2003; Roy & Dun, 2003 Jaiswal et al., 2002).

Here, the first step of the fire management system is fire risk mapping, by analyzing the factors that cause forest fires, predicting fire risk and thus preventing fires and fires damage. For this reason, the creation of forest fire risk and hazard maps constitutes an important basis for preventing fire disaster and damage caused by fire. Pre-fire mapping of fire-sensitive areas, taking necessary precautions in areas with high fire risk , the deployment of first responders, especially in areas that are sensitive to fire at the first degree, facilitates the access of fire crews to the fire as soon as possible by using the shortest and safest way and makes it possible to create the necessary bases for firefighting.

In order to create fire risk maps, it is necessary to reveal and examine the factors that are effective in

***Corresponding Author**
*(firuzaaghayeva.geoph@gmail.com) ORCID 0009-0003-5378-8196

Cite this article
Aghayeva, F. (2023). Wildfire hazard and risk assessment: The case of Gabala district. *Advanced GIS*, 4(1), 01-09.

forest fires. This makes it necessary to evaluate natural and anthropogenic factors together. Land cover especially vegetation represents the combustible material necessary for the emergence and development of fires. The slope factor in natural factors (vegetation, topography) also has an important effect.

In forest fires, the flames can easily reach the areas here by moving rapidly up the slope.Aspect is also one of the important parameters affecting the spread of fires. Generally, south-facing slopes are more susceptible to forest fires than other slopes . Anthropogenic factors, on the other hand, can be explained as the spatial distribution of certain infrastructure facilities used by people such as roads and residential areas, and these factors also affect forest fires . Due to the human factor, the probability of fire in places close to settlements is high.

The main purpose of this article as a result of the created fire risk maps, to contribute to the effective fight against fire by identifying in advance the areas with a high risk of fire and having knowledge about fire behavior.

Research area is located South slopes of Great Caucasus and Qanıx-Ayricay valley. Qabala is old district of azerbaijan. The region is located at an altitude of 68-4466 m. It covers an area of 1,548,600 ha. Forest area occupies 21% of the territory. Fauna and flora species included in the red book of Azerbaijan are spread in the area. Azerbaijan is a country with few forest resources. Forests covered 11% of the country's total area. The south slope of the Greater Caucasus stands out in the country for its percentage of forests (40% of the area) (Məmmədov & Xəlilov, 2022). On the South slopes of Great Caucasus, which is well provided with forest resources, nature protection is considered one of the urgent issues. 45 percent of the territory is occupied by Specially Protected Nature Areas. There are a part of the Shahdag National Park, Gabala and Turyanchay nature reserves, 28 biological nature monuments and specially important forest areas taken under state control in the territory of Gabala region. Despite this, 40% of the fires that occurred on the south slopes of the Greater Caucasus in 2021 and 2022 fall on the territory of Gabala region. During the research period, 1826.3 ha of forest area was burned. This is 5.64% of the total forest area of the district. During the research period, 1826.3 ha of forest area was burned. This is 5.64% of the total forest area of the district. 2021 and 2022 were taken as research years. Wildfire hazard and risk assessment and fire risk zonation of Gabala district was carried out taking into account factors such as anthropogenic and effects of topography. In order to assessment the obtained result, it was compared with the fire data of recent years and the areas covered by the fire.

2. Method

Remote Sensing data programs and ArcGIS map 10.8 Software were used for fire risk assessment in Gabala region during the research (Figure 1).

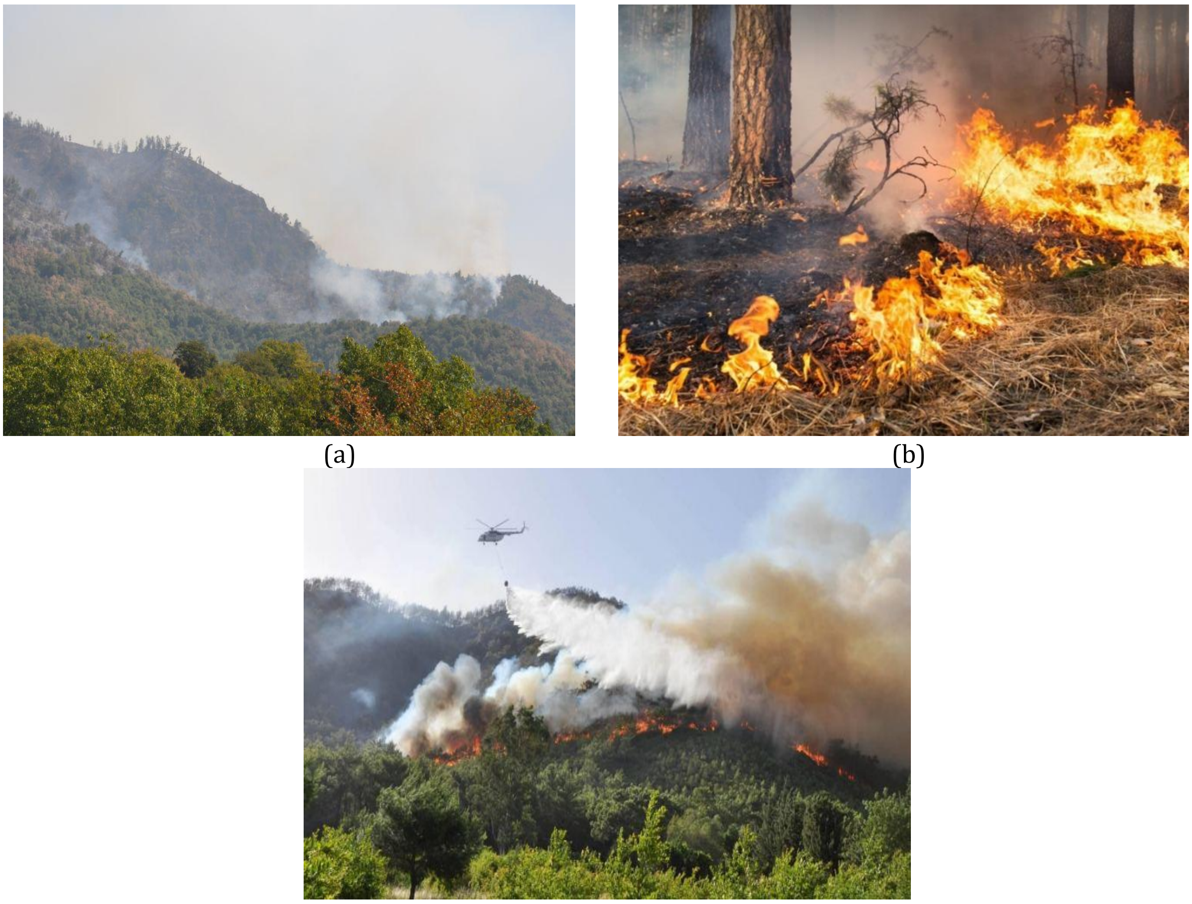

(a) (b) (c)

Figure 1. (a) Gabala district, (b) Gabala district, Solquca village, (c) Gabala district, Tikanlı village

Effects of topography (slope, elevation, aspect) and anthropogenic parameters were taken as criteria. when assessing the fire risk of the area, it is divided into 5 categories; no risk; low risk; medium risk; high risk; critical risk. Here, the slope, elevation, aspect and land use and land cover (LuLc) parameters were reclassified .Then overlay and map algebra operations were performed. Using this information, a fire risk assessment and risk zonation map was created. 30 m resolution SRTM DEM data provided by NASA, USGS were used to study Aspect, Slope and Elevation parameters. To investigate the land use and land cover parameters, the "Landsat 8" data provided by USGS Earth Explorer dated 17.07.2022 was used.

The following steps were taken to create the wildfire hazard risk assessment and zonation map:

- The Aspect layer has been created (Aspect).
- The Aspect layer has been reclassified (Reclassify).
- The Slope layer has been created (Slope).
- The Slope layer has been reclassified (Reclassify).
- The Elevation layer has been created (Elevation).
- The Elevation layer has been reclassified (Reclassify).
- Land use and land cover layer has been created (LULC).
- Land use and land cover layer has been (Reclassify).
- Performed overlay and map algebra operations using elevation, slope, aspect and land use and land cover reclassification layers and was created wildfire risk assessment and zonation layer.
- Wildfire risk assessment and zonation layer has been reclassified.
- Wildfire risk assessment and zonation layer has been converted to a Polygon Layer (Raster to Polygon).
- Wildfire risk assessment and zonation map has been created.
- Wildfire risk assessment and zonation layer has been converted to a Polygon Layer (Raster to Polygon).
- Wildfire risk assessment and zonation map has been created.

Data on wildfires and burned agricultural residues were obtained from the Moderate Resolution Imaging Spectroradiometer (MODIS), a satellite-based sensor. Information about Forest and agricultural resudes active fire location data was taken “NASA FIRMS” application, which is, uses different type of satellite-based sensor (Landsat, VIRS (S-NPP & NOAA 20), MODIS (Aqua & TERRA). Using in this data was created wildfire burned area and active wildfire location map and graphs. In addition, using the existing stock literature materials, information on climate was investigated and certain results were obtained.

3. Results

Based on the effects of topography (slope, aspect, elevation) and Land use and Land cover parameters of the study area, fire risk classification was carried out (Table 1). A fire risk assessment and a zonation map were drawn up according to the obtained categories. As a result, based on the obtained values, overlay and map algebra operations were performed, and the WildFire Assessment and Zonation map was drawn up and the area of the areas included in the risk categories was calculated (Figure 2).

Table 1. Wildfire risk assessment criteria

Risk assessment	Aspect (°)	Slope (°)	Elevation (m)	LuLc
No risk	0-45 315-360	0-8	3500-4466	Water bodies, bare earth, bare soil
Low risk	45-90, 270-315	8-15	3000-3500	Selitep areas
Moderate risk	90-135	15-25	68-500	Agricultur e land
High risk	135-180 225-270	25-35	2000-3000	Pasture
Critic risk	180-225	35-68	500-2000	Forest

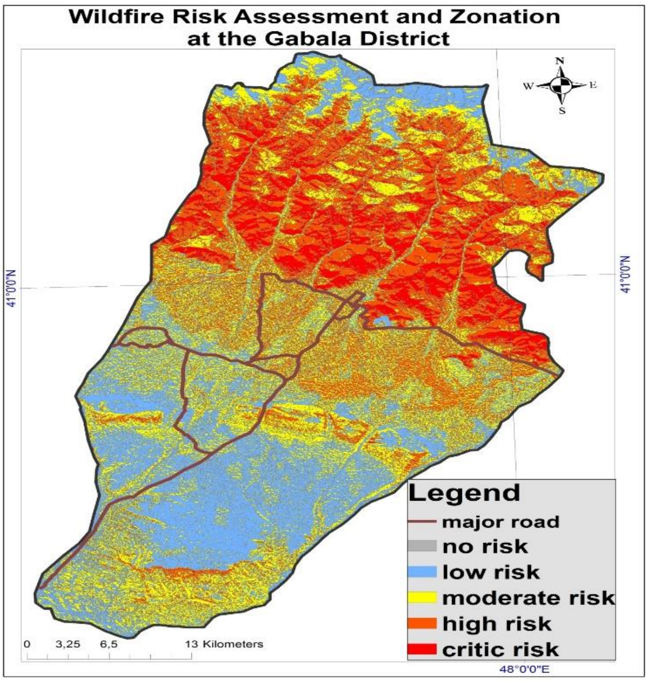

Figure 2. Wildfire risk assessment and zonation

In general, 0.43% of the territory corresponds to no risk, 28.24% to low risk, 35.01% to moderate risk, 24.48% to high risk, and 10.84% to critical risk classification (Figure 3).

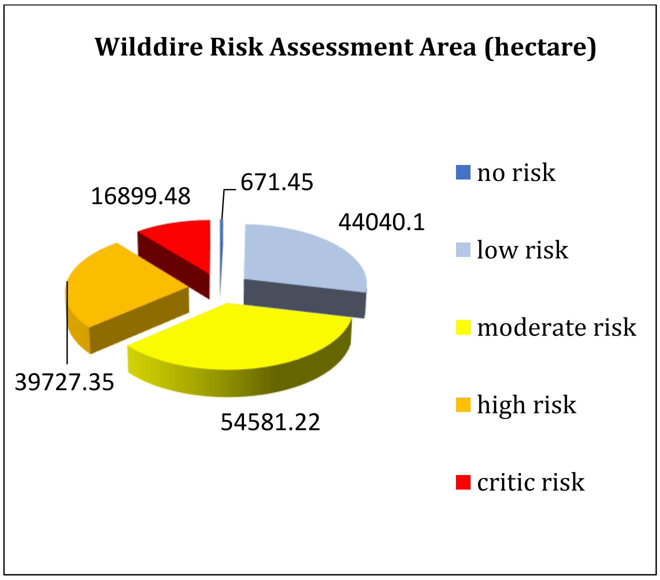

Figure 3. Wildfire risk assessment area (hectare)

The resulting values were classified according to the risk group and the results were compared with the fire area data. In total, 108 fire incidents occurred in the area in 2021 and 11 in 2022 year. As a result of the comparison, no fire process was found in the non-risky area. There were 2 fire incidents in the low risk category, 10 in the moderate risk category and 107 in the high and critical risk categories. Thus, we can see that 90% of fire incidents correspond to the high risk and critical risk category (Figure 4).

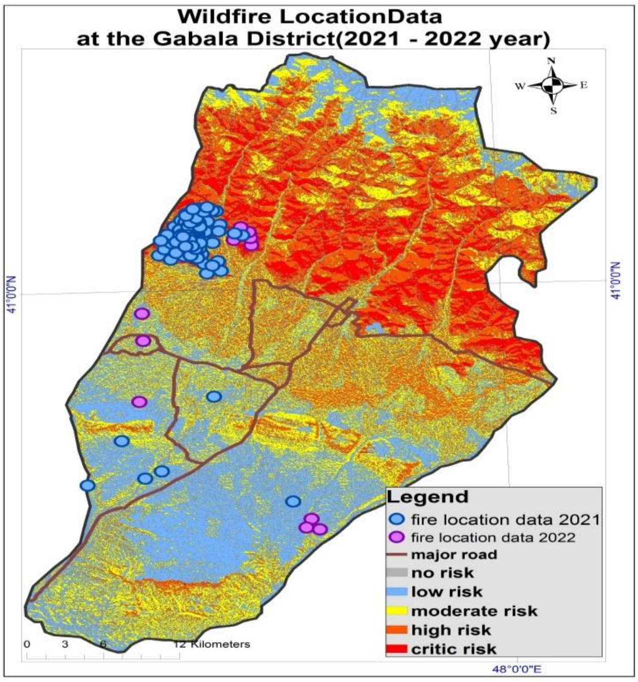

Figure 4. Wildfire location data (2021-2022 year)

When the obtained results are compared with the fire area data, we can see that 100% of the area corresponds to the high risk and critical risk category. In general, during the study period, it was determined that 5.4% of the forest resources were destroyed based on the fire area data (Figure 5).

It is extremely important to be able to predict the potential fire risk and fire hazard of a region in forest fire fighting studies. In this way, potential areas with high fire risk and danger will be given priority in pre-fire planning, and protective and preventive measures will be handled more comprehensively in these areas. In this context, making the area safer in terms of forest fires by reducing the risk and danger of fire will be possible. Similarly, in order to effectively fight possible fires, these areas where the fire risk and danger are high should be given priority in the deployment, management and administration of resources and teams.

In these results, it is an indication that the selected parameters and the evaluation are reasonable.

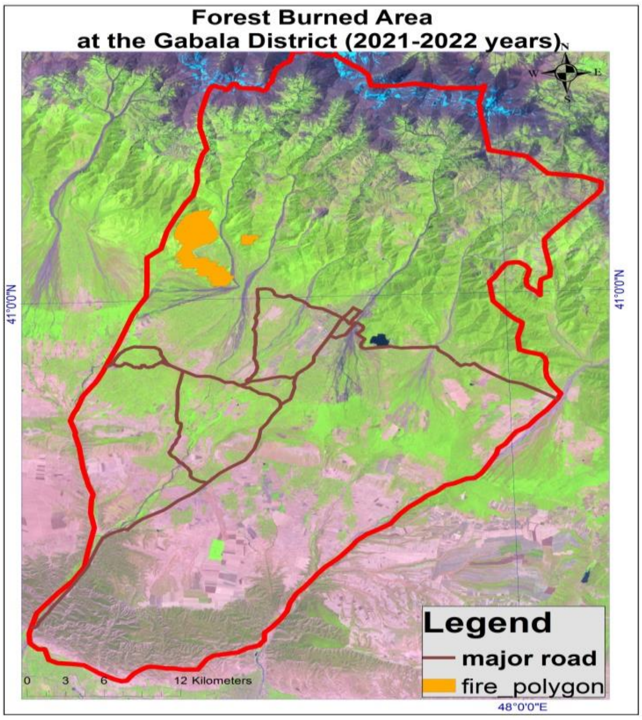

Figure 5. Forest burned area (2021-2022 year)

4. Discussion

As one of the main natural resources for humans, protection of forest resources is one of the main ecological problems of the world. Forests are a source of oxygen, as well as they have some features that can ensure ecological balance. For example, forests are one of the major factors that prevent landslides, erosion processes, flood events, as well as protecting land resources, hydrological resources and optimization micro climatic condition. Decreasing of forest stock affects the fauna directly. There are some factors that impact decreasing of forest resources, for example, settlements, industry and forest supply and etcetera. Forest fires occurring in different parts of the world every year eradicated acres of forest stock. Willdfires formed in 3 different ways.

- Cover fire
- Hill fire
- Ground fire

Cover fire; It is produced by the burning of needles, branches, cutting residues, grass, heather and live cover on the forest floor. It rarely harms the native tree species of the forest. When the weather is humid and in the winter months, it turns into hill fires.

Hill fire: Damages the entire forest, especially the original tree species in the forest. It is a type of fire that burns the tops of trees. When we say hill fire, it should be understood that all the elements in the forest, including the substances on the soil surface, are burned.

Ground fire: Fires that occur in peat above and below (the root part) of forest soil, such as marshes and bogs.

Wildfires that have been in Gabala district area are basically suitable for the 1st group. Here, wildfire, which are characterized as hill fire, also occur. But wildfires such as ground fire do not occur here.

On 16.08.2021 and 26.08.2021 Solguca, on 08.08.2021 and 03.04.2022 in Vandam, on 16.08.2022 Abrikh and Tikanlı, on 01.09.2022 in Tikanlı the mountain forest area near the can be attributed to group 1 forest fires (Figure 6). During the incident, dry grass, bushes, dried tree stumps and some trees burned in the forest area.

On 11.08.2021, the forest fire that started on the Kyzylburun mountain near Tikanlı village spread to the territory of the Ganjadash mountain under the influence of strong wind and covered an area of more than 50 ha. It also destroyed dry grass, bushes, dry trees, their remains and trees. . This fire can be attributed to the ground fire type.

On 04.09.2021, the forest fires that lasted for more than 20 days near the villages of Solguca, Dandikh, Abrikh and Tikanli spread to the territory of the Shahdag National Park. The forest fire that happened here can be attributed to the 2nd group according to its nature.

In total, 1826.3 ha of forest area was burned during 2021 and 2022. Forest restoration works have been carried out in these areas.

A partial middle and high zone of forests in Gabala District is included in the territory of Shahdag National Park. Any interference in the national park territory is prohibited according to the regulations of specially protected natural areas.For this reason, dry trees in the territory of the National Park are not touched. Dry firewood increases the likelihood of transition from a surface fire to a hill fire. Given that the area is included in the critical risk classification, dead trees and their remains are likely to exacerbate the danger during a fire. In this regard, in the last 3 years, the process of collecting dead trees in the territory of the National Park has been started.

The formation of forest fires is influenced by factors such as climate, anthropogenic and topological effects. Research area is district of Gabala which is situated at south slopes of Greater Caucasus. Gabala is distinguished by the abundance of forest resources in the territory of Azerbaijan, which is poorly provided with forest reserves. In the north of Gabala, alpine and subalpine meadows, mountain forests, bushy and sparsely wooded meadows in the central part, and wormwood and wormwood-saline semi-desert plants, xerophytic sparse forests occupy a large area. It is an area with high tourism potential. It has a dense river network system (Türyan, Demiraparan and their tributaries Tikanlıchay, Bum, Vandam, etc.).

When assessing the occurrence and spread of forest fires, it is important to consider parameters such as climate, anthropogenic and effects of topography. In this article, the classification was made mainly based on anthropogenic and relief factors. The following table lists the parameters of the classification and the results of research conducted based on these parameters in the area.

Table 2. Areas calculated based on wildfire risk assessment criteria (area values hectare)

Risk assessment	Aspect area	Slope area	Eleva-tion area	LuLc cover area
No risk	3414.90	74666.70	2032.70	20802.20
Low risk	395550.70	19792.90	6413.82	32495.19
Moderate risk	15961.10	24991.20	58011.60	24395.95
High risk	47370.80	25011.10	12593.30	46371.68
Critic risk	28897.60	11459.80	42198.30	32405.15

Climate factor. The climate is mild-warm with dry winters in the lower part, and cold and humid in the highlands. Annual precipitation is 500-600 mm in the lower part, up to 1600 mm in the highlands. Average monthly temperature decreases with increasing altitude. While the average temperature in July is 24-27 C° in the plain part of the region, it drops to 20-15 C° in the middle highlands, and 10-5 C° in the highlands. While the average January temperature is 2 C° in the plains, it drops from -10-(-11) C° to even -14-(-15) C° in the high mountain peaks. Taking into account climate parameters (temperature and humidity), the risk of fire decreases with increasing altitude. The increase in temperature in the summer months and the partial decrease in precipitation increase the risk of fire. During the research period, according to the data we took from the "NASA FIRMS" platform, it can be seen that 93.27% of fire incidents happened in the summer months (August, early September). It should be noted that the fire events that occurred in September coincided with the first 5 days of the month (Müseyibov, 1998).

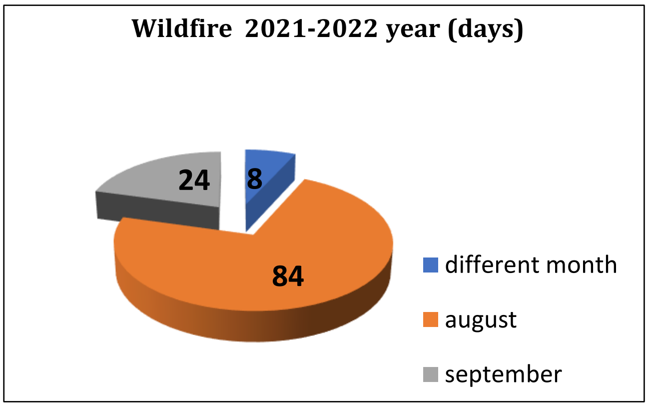

Figure 6. Wildfire events 2021-2022 year (days)

The causes of fires are mainly to combine under 3 groups: unknown, natural and anthropogenic factors.

1-Unknown:

These are fires whose origin is unknown.

2-Natural Fire:

These are fires that occur without any human factor. These are fires that started due to lightning, volcanic activities and gas emissions.

Lightning: Fires caused by lightning strikes.

Volcanic activities: These are fires originating from volcanoes.

Gas Emission: These are fires that occur spontaneously as a result of the compression of gases. Spontaneous ignition of underground mines and burning of garbage cause forest fires.

3- Anthropogenic factors are one of the main factors we should pay attention to when assessing fire risk. A number of anthropogenic effects, which we have listed below, cause forest fires.

- carelessness, negligence and intentional burning.
- making campfires in the forest without observing safety rules
- Throwing unextinguished cigarette butts and matches on the ground
- throwing glass and broken glass into the forest
- stubble burning
- intentional fires

The distance from residential areas and highways was taken into account when assessing the risk. Looking at the map of highways in Figure 3, it is clear that most of the fires classified as moderate risk occur in the buffer zone of 2000 m, which is defined as a risk area. (Figure 7).

The fires in Gabala are mainly anthropogenic in nature. The main cause of anthropogenic forest fires are careless and intentional fires. Fires caused by carelessness have increased in recent times in connection with the rapid development of tourism in Gabala region. The increase in the number of tourists in the area, their use of forests without complying with safety rules, causes fires. Unextinguished cigarette butts are thrown into the forest, barbecues are left in the forest area, bonfires are left in picnic areas, and bright materials are thrown into the forest due to carelessness.

Attributing the following to other fires caused by negligence:

- vegetation management: Non-agricultural vegetation management fires caused by unintentional burning.
- Agricultural Activities: Plant wastes (Example stubble) fires caused by burning.
- Waste management (dump): Official or illegal dumping of waste fires caused by burning.

Forest fund territories are bordered by municipally owned lands and farms. Burning of stubbles after grain harvesting, careless handling of fire in pastures (the road to pastures passes through the territory of the forest fund) and other similar cases eventually lead to the spread of fires to forests.

The reason for the fire that occurred near Yenikend village on 03.04.2022 is that the fire spread to the forest area during the burning of garbage in the backyard of the villager.

Another cause of forest fires that occur in the area of Gabala is intentional. There are 3 settlements and 60 villages in the territory of Qabala district, of which 29 villages are not gassed. In winter, the population's demand for fuel leads to the use of forest resources as firewood. Since the wood is mainly grown in Azerbaijan, the broccolis burn the trees that are cut down to hide their activities. Some of these activities are observed more intensively in the regions of Tikani, Abrix, Solquca and Dandıq, which are not yet fully met. 89% of the oak burns that broke out in 2021-2022 occurred in these areas.: Fires caused by the deliberate burning of forests by people.

- Responsible: These are forest fires started by people over the legal age limit. These fires are examined in seven subgroups.
- Annuity: The reason for exit is to earn money or another way.
- forest fires for the purpose of.(Trench)
- Dispute: The reason for the exit is the fires that were started to take revenge and revenge.
- Vandalism: Malicious mischief and deliberate fires by people with personality disorders.
- Excitement: a sense of people feeling important
- caused by fires.
- Crime concealment: The reason for the fire is to hide a criminal activity.
- Extremism: Fires started for social, political or religious reasons

Intentional wildfire are made in the Gabala district. In Gabala district, there are 28 villages that are not supplied with gas. The cold winter and the population's demand for fuel lead to the use of forest resources as firewood. Since the forests is mainly protected in Azerbaijan, the broccolis burn the area which is trees that are cut down to hide their activities. Some of these activities are observed more intensively in the regions of Tikani, Abrix, Solquca and Dandıq, which are not supplied with gas. 89% of the wildfire that broke out in 2021-2022 occurred in these areas.

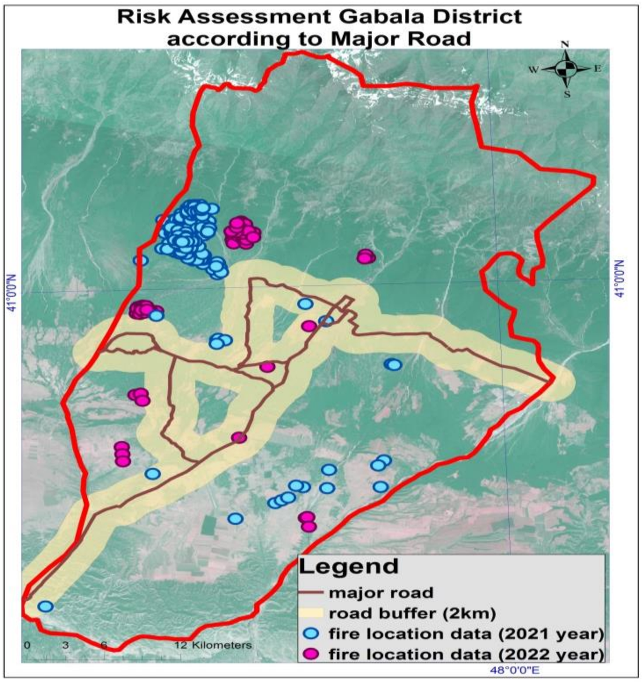

Figure 7. Risk Assessment according to major road.

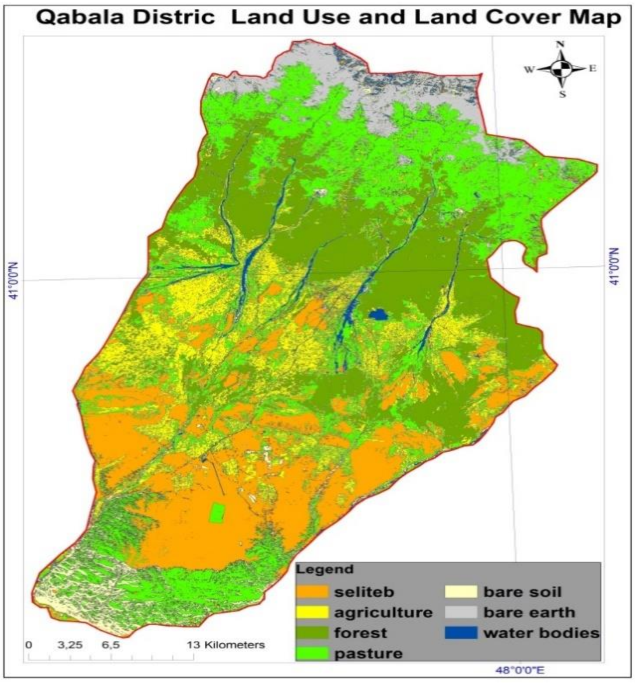

Figure 8. Land use and land cover

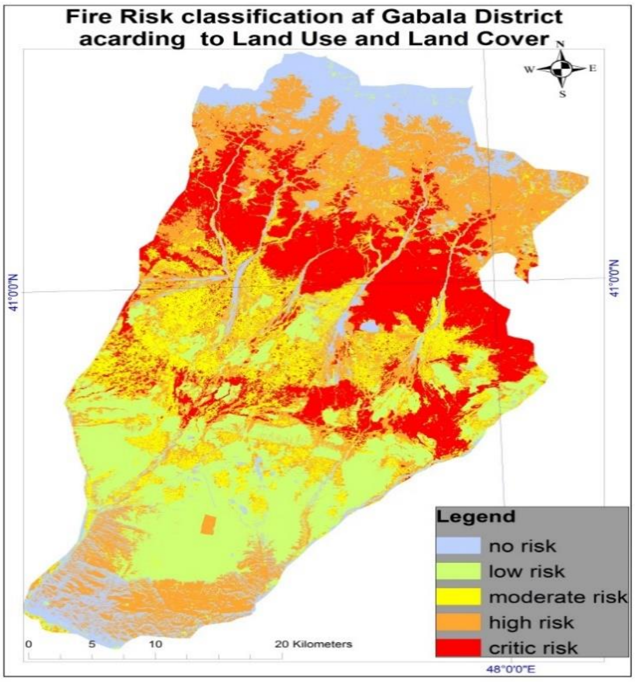

Figure 9. Fire risk classification acording to land use and land cover

The settlement factor was taken into account during the research. After the 2000s, the rapid development of tourism in the region has led to an increase in anthropogenic loads in the area. Resort-recreation centers created in the forest area increase the risk of forest fires of anthropogenic origin. As we can see in Figure 8, the central part of the area (200-800 m) is more densely populated. This corresponds to the lower border of the forest. Settlements exist in the middle forest (800-1200 m) zone.

The map was prepared using arcgis 10.8 software from Landsat 8 data dated 17.07.2022 provided by USGS EarthExplorer. At this time, forest, agriculture land, urban areas, pastures, bare soil and earth land areas were classified using 1, 2, 3, 4, 5, 6, 7 band combinations and a land use and land cover map was drawn up. The resulting values were classified according to the risk group. The forest area of the total area is 20.71%. Settlement and appropriated areas cover 36.36%, summer and winter pastures cover 29.64%. In general, it is classified as water bodies, bare earth and soil land no risk, selteps low risk, agricultural area medium risk, pastures high risk, forest critical risk. In Figure 8, the Land use and Land cover map of the area was drawn up, then fire risk classification was made based on it (Figure 9).

Elevation, slope and aspect parameters of the area are the main relief features that affect the risk of forest fires (Castro & Chuvieco, 1998; Chuvieco & Salas, 1996). It provides important information about the determination of the fire area, the speed and direction of its spread. Assuming other risk factors are constant, fire will move fastest on steep slopes. That said, increased inclination also increases the risk of fire.

The territory of Gabala district has an inclination interval of 7° - 68°. The inclination increases from south to north. 5 classifications were used when assessing forest fire risk based on slope inclination: 0-8° no risk, 8-15° low risk, 15-25° medium risk, 25-35° high risk and 35-68° critical risk areas. 47.9% of the total area of the territory is classified as no risk, and 23.4% as high and critical risk (Figure 10).

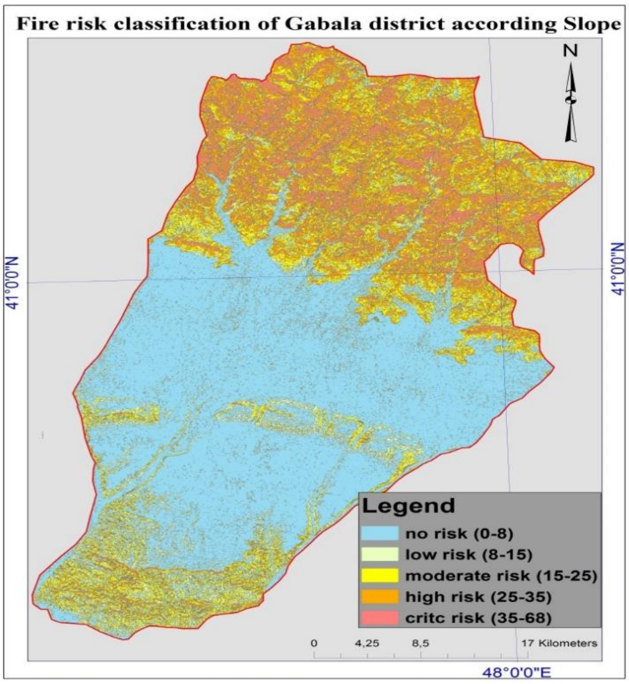

Figure 10. Fire risk classification according slope

Although the angle is fixed, the received solar radiation varies according to the position of the sun. Therefore, the strong influence of sun exposure on fire behavior varies throughout the day. The amount and type of fuels available varies greatly by tank.

North slope: Compared to other slope, the sunbathing time is less. It is advantageous in terms of fires. However, the humus layer is thicker.

South slope: They spend a long time in the sun, they are exposed to higher temperatures during the day. Eastern slopes: slopes are the first to receive the sun during the day. It is less sensitive than the south and west. Western slopes After South slope, they have the most sunshine time and are dangerous in terms of forest fires

Fire conditions vary greatly depending on the aspect. In general, the south and southwest sides have good conditions for fire initiation and spread. These areas receive more sunlight. Increases the temperature of air and combustible material. (Figure 11).

7.35 percent of the area corresponds to critical risk, 16.04 percent to high risk, 16.03 percent to moderate risk, 12.69 percent to low risk, and 47.89 percent to no risk classification.

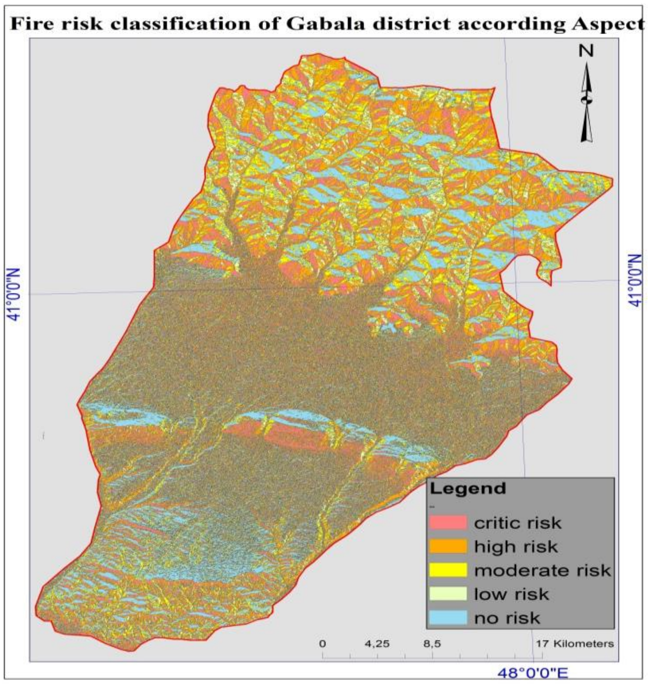

Figure 11. Fire risk classification according aspect

Elevation data is closely related to the distribution of vegetation. Vegetation in the study area is distributed along the vertical zonation of the mountainous area. Bushy and sparse meadows are spread in the central part, and semi-desert plants with wormwood and sorrel in the south, and arid type forests in the steppe plateau area. At altitudes of 600-2000 m, there are oak, beech and walnut forests. Subalpine (1700-2600 m) and alpine meadows (2500-3100 m) are common in the high mountain zone. At 3100-3500 m above sea level, subnival plants of the tundra type are found. Above 3500 m, the vegetation-free nival zone begins. Taking these into account, Elevatian classification was made again. Areas with an altitude of 500-2000 m are classified as critical risk zone, while areas higher than 3000 m are included in no-risk and low-risk categories (Figure 12).

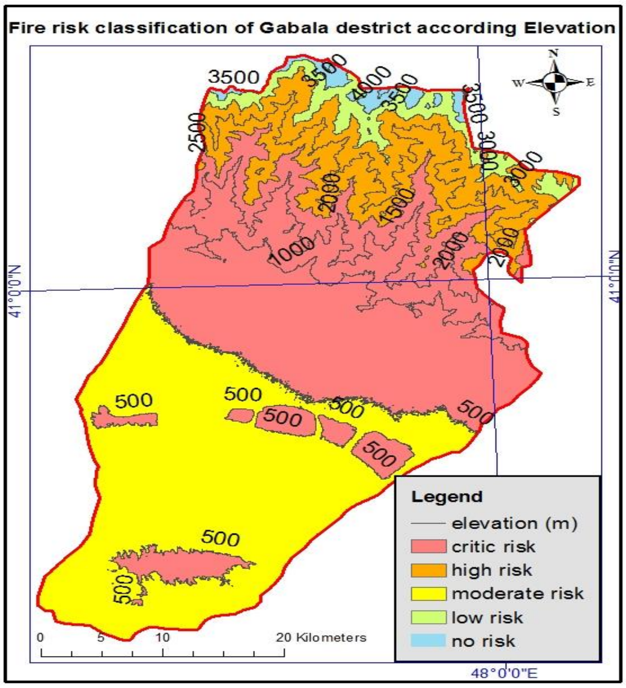

Figure 12. Fire risk classification acording elevation

5. Conclusion

Burned area data was used to verify the obtained data. The data is taken from the FIRMS database with 1000 m resolution from MODIS/MOD 14 sensors from the earth.data.nasa.gov application. Vectorized and area calculated using ArcGis 10.8 software. Data covers 2021 and 2022. The burnt forest area is 1826.3 ha, which is 5.4% of the forest area of Gabala district. 100 percent of the burned area corresponds to the high and critical risk classification zone. 2021 and 2022 data from MODIS (Aqua and Terra) sensors provided by NASA FIRMS are taken. In Gabala district, 11 fire incidents occurred in 2021 and 108 in 2022. 90% of recorded fire events correspond to the high and critical risk classification area, 8.4% to the moderate risk zone, and 1.6% to the low risk zone.

It is extremely important to be able to predict the potential fire risk and fire hazard of a region in forest fire fighting studies. In this way, potential areas with high fire risk and danger will be given priority in pre-fire planning, and protective and preventive measures will be handled more comprehensively in these areas. In this context, making the area safer in terms of forest fires by reducing the risk and danger of fire will be possible. Similarly, in order to effectively fight possible fires, these areas where the fire risk and danger are high should be given priority in the deployment, management and administration of resources and teams.

Author Contributions

The article was carried out by a single author.

Statement of Conflicts of Interest

There is no conflict of interest.

Statement of Research and Publication Ethics

Research and publication ethics were complied with in the study.

References

Atun, R., Kalkan, K., & Gürsoy, Ö. (2020). Determining the forest fire risk with Sentinel-2 Images. Turkish Journal of Geosciences, 1(1), 22–26.

Bar, S., Parida, B. R., Pandey A.C. (2020). Landsat-8 and Sentinel-2 based forest fire burn area mapping using machine learning algorithms on GEE cloud platform over Uttarakhand, Western Himalaya. *Remote Sensing Applications: Society and Environment,* 18, 100324. https://doi.org/10.1016/j.rsase.2020.100324

Başaran M. E., Sarıbaşak H., & Cengiz Y. (2004). Yangın söndürme temel esaslarının belirlenmesi (Manavgat Örneği). *Batı Akdeniz Ormancılık Araştırma Müdürlüğü Teknik Bülten,* (18), 1-96.

Başkent E. Z. (2018). A review of the development of the multiple use forest management planning concept, *International Forestry Review,* 20(3), 296-313. https://doi.org/10.1505/146554818824063023

Betanzos, A. A., Romero, O. F., Berdinas, B. G., Pereria, E. H., Andarade, M. I. P., Jimenez, E., & Soto, J. L. L., Carballas, T. (2003). An intelligent system for forest fire risk prediction and fire fighting management in Galicia. *Expert Systems with Applications,* 25(4), 545-554. https://doi.org/10.1016/S0957-4174(03)00095-2

Castro, R., & Chuvieco, E. (1998). Modelling forest fire danger from GIS, *Geocorta International*, 13(1) 15-24. https://doi.org/10.1080/10106049809354624

Chuvieco, E., & Salas, F.J. 1996, Mapping the spatial distribution of forest fire danger using GIS. *International Journal of Geographical Information Systems,*10, 333-345. https://doi.org/10.1080/02693799608902082

Dong, X., Shao, G., Limin, D., Zhanging, H., Lei, T., & Hui, W. (2006). Mapping forest fire risk zones with spatial data and principal component analysis. *Science in China: Series E Technological Sciences,* 49(Supp. I), 140-149. https://doi.org/10.1007/s11434-006-8115-1

Goldammer, J. G., & Mutch, R. W. (2001). *Global forest fire assessment FAO forest resources assessment programme, working paper* 55. Retrieved July 13, 2023, from https://www.fao.org/3/AD653E/ad653e00.htm

Jaiswal, R., Mukherjee, S., Raju, K., & Saxena, R. (2002) Forest fire risk zone mapping from satellite imagery and GIS. *International Journal of Applied Earth Observation and Geoinformation*, 4(1), 1-10. https://doi.org/10.1016/S0303-2434(02)00006-5

Kuter, N., Yenilmez, F., & Kuter, S. (2011). Forest fire risk mapping by kernel density estimation. *Croation Journal of Forest Engineering*, 32(2), 599-610.

Məmmədov, Q., & Xəlilov M. (2022). *Azərbaycan meşələri.*

Müseyibov, M. (1998). Azərbaycanın fiziki coğrafiyası. *Maarif Yayınları*, 127-131.

Roy, P. S. (2003). Forest fire and degradation assessment using satellite remote sensing and geographic ınformation system. *Satellite Remote Sensing and GIS Applications in Agricultural Meteorology* pp. 361-400.

Versini, P., Velasco, M., Cabello, A., & Sempere-Torres, D. (2013). Hydrological ımpactof forest firesand climate change in Mediterranean Basin. *Natural Hazards*, 66 (2), 609-628. https://doi.org/10.1007/s11069-012-0503-z

Advanced GIS

http://publish.mersin.edu.tr/index.php/agis/index

e-ISSN:2822-7026

Comparative evaluation of the performance of different regression models in land valuation

Sukran Yalpir*[1], Erol Yalpir [2]

[1]Konya Technical University, Faculty of Engineering and Natural Sciences, Department of Geomatics Engineering, Konya, Türkiye
[2]Konya Provincial Directorate for National Education, Yazır Şehit Osman Küçükdillan Primary School, Selçuklu/Konya

Keywords
Land Valuation,
Lasso,
Elastic-Net,
ML.Net,
OLS Regression

check for updates

Research Article
Received: 18/01/2024
Revised: 02/02/2024
Accepted: 07/02/2024
Published: 02/04/2024

Abstract

Lands can play a dominant role in the real estate market, especially due to their legal zoning rights. These properties are preferred investment options compared to financial instruments due to factors such as high returns and long-term reliability. Today, Machine Learning (ML) algorithms are used to accurately determine the land value. Regression models, capable of handling complex relationships, integrating Geographic Information System (GIS), and providing a comparative approach, lead the way among these algorithms. In this study, Lasso, Elastic-Net, ML.Net, and Ordinary Least Squares (OLS) regression models were employed to predict land values in the central neighborhoods of Konya's Selçuklu, Meram, and Karatay districts. The datasets containing legal, physical, spatial, and local criteria of 440 lands were obtained, and GIS analyses were conducted to prepare the spatial data. Based on the modeling results, it can be observed that ML.Net exhibited successful performance with metric values of MAE=0.043, MSE=0.005, RMSE=0.060, and R2=0.82. Comparatively, ML.Net's 9% superior performance compared to the commonly encountered OLS in the literature is of significant importance. The results demonstrated the usability of various regression models for land valuation and highlighted that ML.Net can yield improved outcomes, particularly in modeling high-market-value lands.

1. Introduction

Quantitative determination of the value of the residential zoned lands, which are the basic building blocks of today's cities, with popular approaches and sustainable land management is of great importance. (Demetriou, 2016; Derdouri & Murayama, 2020). Lands can play a dominant role in the real estate market in developing cities, especially due to their legal zoning rights. They are among the most preferred investment items due to factors such as higher return amount and reliability compared to financial investment items such as foreign currency and stocks, and not losing value in the long run.

Lands, like other types of real estate, have many criteria that affect the value. Although it is very difficult to group these criteria, criteria can be defined in four main groups. These groups can be defined as legal, physical, spatial and local, respectively. The legal criteria group defines the criteria such as Base Area Coefficient (BAC), Floor Area Coefficient (FAC), and number of floors, which define the zoning status of the lands in terms of planning. The physical criteria group defines the criteria that express the situations such as the geometric shape of the land and the benefit from the infrastructure elements. The spatial criteria group defines the characteristics that define the effects of distance to urban points of interest such as education, health, and transportation on land value. The local criteria group, on the other hand, defines the characteristics that represent the social structure such as the education level of the people living in the region where the land is located, the population density, and the environmental criteria that have an effect on the land value such as air quality and noise pollution (Hu et al., 2016; Doan, 2023).

Therefore, the objective and criteria-based determining the land value with popular approaches such as Machine Learning (ML) algorithms has opened new horizons for many transactions from taxation to expropriation, from urban transformation to capital market activities (Krause & Bitter, 2012; Sisman & Aydinoglu, 2022). The usage of regressions in ML stands out as an effective approach for determining land values. Regression models can handle more complex relationships, while the integration of Geographic Information System (GIS) can enhance predictions by incorporating spatial data. Models based on linear or non-linear regression constitute one of the most commonly used approaches in practical implementation of statistical analysis of the market within a comparative approach for land valuation (Foryś & Gaca, 2018; Kokot & Gnat, 2019). In the literature, it is seen that the results obtained in the regression-based land value estimation give better results than the models based on other approaches (Zurada et al., 2011).

***Corresponding Author**

*(syalpir@ktun.edu.tr) ORCID 0000-0003-2998-3197
(eyalpir@gmail.coml) ORCID 0009-0002-9312-4354

Cite this article

Yalpir, Ş. & Yalpir, E. (2024). Comparative evaluation of the performance of different regression models in land valuation. *Advanced GIS,* 4(1), 10-14.

Within the scope of this study, as a part of land management and valuation, ML models were implemented in the central neighborhoods of Konya's Selçuklu, Meram, and Karatay districts. In the modeling process; Lasso, Elastic-Net, ML.Net and Ordinary Least Squares (OLS) regression models were used together with legal, physical, spatial and local criteria affecting the land value. The datasets were organized for the market values, properties and spatial features of 440 land offered for purchase/sale. The valuation of land-type real estate with GIS-integrated use of different methods has been realized. Results obtained from the models were compared according to the performance metrics such as determination coefficients (R^2), Mean Absolute Error (MAE), Mean-Square Error (MSE), and Root-Mean-Square Error (RMSE).

2. Materials and Methods

2.1. Study area and dataset

Neighborhoods in Selçuklu, Meram, and Karatay districts, which are among the central districts of Konya city, were determined as the study area. In the determination of the study area, the location of the land-type real estate in high market activity were taken into consideration. As seen in Figure 1, the study area also includes many urban service functions such as education, industry, agriculture and transportation facilities. All these factors were effective in determining the study area.

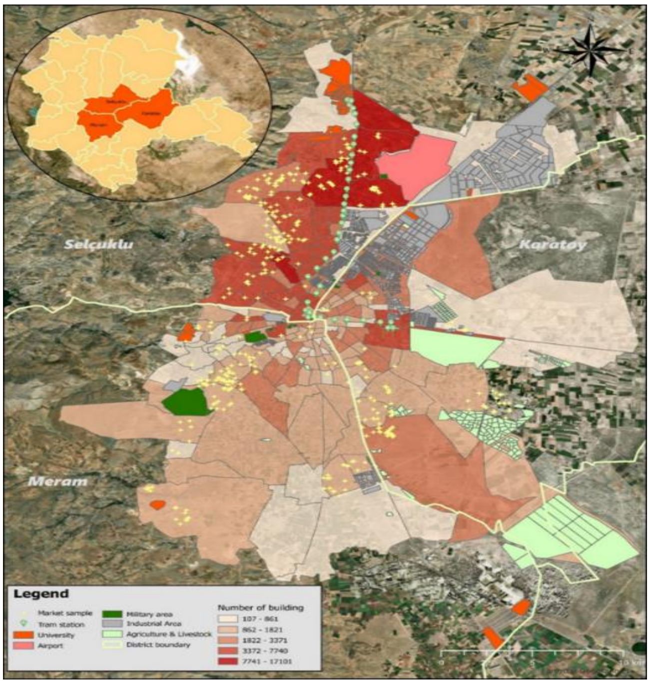

Figure 1. Determining the study area and distribution of market samples

A total of 440 market samples within the study area and geographical data representing legal (5), physical (6), spatial (11) and local (9) criteria affecting the land value were obtained. All data were organized in a GIS environment. Relationships between market samples and geographic datasets were defined. In this context, the geographical distribution of the market samples is presented in Figure 1, and summary statistics on some numerical legal and physical variables in the dataset are given in Table 1.

Table 1. Summary statistics about some numerical variables in the dataset

Variable	Min.	Max.	Mean	Standard Deviation
Market value (₺)	550000	23500000	3339727	3458173
BAC	0.08	0.90	0.24	0.07
FAC	0.15	3.60	0.59	0.34
Number of floors	1.00	8.00	2.44	0.90
Area (m²)	117.00	5462.00	875.20	648.11
Facade length (m)	4.00	100.00	25.41	13.43
Number of facades	1.00	4.00	1.47	0.62
Road with (m)	4.00	40.00	11.87	4.70

Then, the local influence distances for each of the spatial criteria were defined by literature research as given in Table 2. Each criterion was analyzed by using its related distance values. The maps of the analysis results for some criteria such as distance to transportation, city center, shopping center and green areas are given in Figure 2. In this way, the analyzes of all criteria were completed and the results were spatially brought together with market samples. Thus, an enriched dataset was prepared for modeling studies.

Table 2. Buffer distances for spatial criteria (Sisman et al., 2023)

Spatial criteria	Analysis Distance (m)
Distance to healthcare facilities	250-500-750-1000-1250
Distance to education facilities	750-1000-1500-2000-2500
Distance to public agencies	1000-2000-3000-4000-5000
Distance to security units	1000-2000-3000-4000-5000
Distance to shopping malls	500-1000-1500-2000-2500
Distance to cultural facilities	250-500-750-1000-1250
Distance to entertainment facilities	500-1000-1500-2000-2500
Distance to green areas	750-1500-2250-3000-3750
Distance to transportation facilities	600-1200-1800-2400-3000
Distance to insanitary areas	250-500-750-1000
Distance to city center	1000-2000-3000-4000-5000

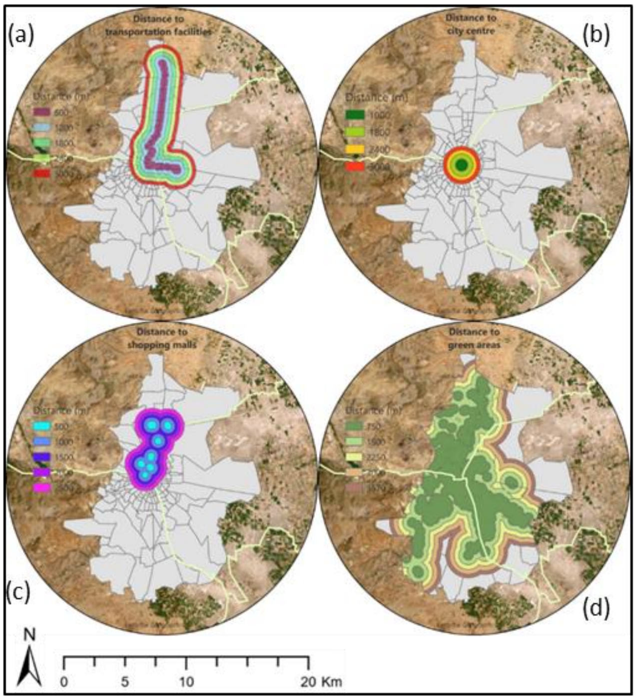

Figure 2. Examples of spatial buffer analysis for (a) distance to transportation, (b) city center, (c) shopping center and (d) green area criteria

2.2. Lasso regression

Lasso is a method used in regression analysis, particularly aimed at reducing model complexity, eliminating unnecessary variables, and preventing overfitting. Essentially, it aims to simplify the model by driving the coefficients of irrelevant variables closer to zero. This method is especially employed in high-dimensional data to diminish the impact of irrelevant features and enhance the model's generalization ability (Tibshirani, 1996). The mathematical equation for Lasso regression is as follows (Equality 1):

$$\mathrm{Lasso} = \sum_{i=1}^{n}(y_i - \hat{y}_i)^2 \; + \; \lambda \sum_{j=1}^{p} |\beta_j| \tag{1}$$

where:

y_i and $\hat{y}_i$ are the observed and predicted values,

λ: Regularization parameter. This parameter controls the complexity of the model and encourages coefficients to approach zero.

$\sum_{j=1}^{p} |\beta_j|$: Using the L1 norm, it represents the sum of the absolute values of all coefficients. This part constitutes the fundamental property of Lasso as it performs variable selection by driving coefficients towards zero.

2.3. Elastic-Net regression

Elastic-Net regression, developed by Zou & Hastie (2005), builds upon the Ridge and Lasso regression methods. Similar to Ridge regression, the correction process is carried out by following the same procedural step. The λ2 parameter applies correction to the β coefficients based on the role of each coefficient in the sum of squared errors. Variable selection is performed similar to the Lasso regression. The coefficients of insignificant variables are set to zero, thus achieving automated variable selection. The equation for Elastic-Net regression is as follows (Equality 2):

$$ElasticNet = \sum_{i=1}^{n}(y_i - \hat{y}_i)^2 + \alpha\left[\frac{1}{2}(1-\lambda_2)\sum_{j=1}^{p}\beta_j^2 + \lambda_1\sum_{j=1}^{p}|\beta_j|\right] \tag{2}$$

where:

n is the number of data points,

p is the number of features,

y_i and $\hat{y}_i$ are the observed and predicted values,

β_j are the regression coefficients,

α is a parameter controlling the regularization,

λ is a parameter controlling the balance between L1 and L2 regularization.

Elastic-Net regression is often effective when dealing with feature selection or datasets with multicollinearity. However, proper tuning of regularization parameters like λ and α is crucial. These parameters can be determined using hyperparameter tuning techniques.

2.4. ML.Net model

ML.Net is an open-source machine learning framework developed by Microsoft. ML.Net allows .Net developers to add machine learning capabilities to their applications while continuing to utilize the .NET platform. It supports various machine learning tasks such as image recognition, natural language processing, classification, regression, clustering, and many more (Ramel, 2018).

Resources and examples related to ML.Net can be found in Microsoft's official documentation as well as in resources provided by the open-source community. ML.Net can assist both novice and experienced developers in easily developing machine learning projects within the .Net ecosystem (Microsoft, 2018).

2.5. Ordinary least squares (OLS) regression

OLS is a statistical method and one of the fundamental techniques in linear regression analysis (Dismuke & Lindrooth, 2006). Its objective is to model the relationship between one or more independent variables and a dependent variable. This relationship is expressed using a linear equation (Equality 3):

$$Y_i = \beta_0 + \beta_1 X_{i1} + \beta_2 X_{i2} + \cdots + \beta_k X_{ik} + \varepsilon_{ij} \tag{3}$$

Y_i is the dependent variable (the value to be predicted). Xik, are the independent variables. βi are the regression coefficients and εij is the error term. OLS aims to predict these coefficients based on a given dataset. The predicted coefficients are calculated to minimize the sum of squared errors. Hence, it's often referred to as the "Least Squares Method".

3. Findings

In the study, the data of 31 variables that affect the land value were organized, and the performance of Lasso, Elastic-Net, ML.Net, and OLS regression models were evaluated. The total number of market samples used for the modeling stage was 440. To achieve high-performance results from the models, the model needed to be trained.

This means that approximately 80% of the dataset was used for training the models, while the remaining portion was used for testing. Optimization was performed to determine the most suitable parameters for each model, and hyperparameter tuning was conducted using 10-fold cross-validation. Table 3 presents the optimal parameters of the regression-based approaches used for land value prediction.

Table 3. Optimal hyperparameters of the various regression models

Model type	Hyperparameters	Optimum value
Lasso Regression	λ	0.004
Elastic-Net Regression	λ_1	0.355
	λ_2	0.331
ML.Net Regression	*Learning_rate*	0.009
	Max_depth	3
	Min_samples_leaf	2
	Other parameters	default
OLS Regression	*Coefficients (Intercept)*	-0.2438
	Other parameters	(31 variables coefficients)

In Table 3, it can be observed that the parameter to be determined for Lasso regression is the λ parameter. According to the analysis results, when the optimum value of λ is 0.004, it implies that the model is most successful under these conditions. In other words, it has been concluded that Lasso regression should be trained with the parameter "λ=0.004".

As for the Elastic-Net regression model, the parameters that need to be determined are λ1 and λ2. Here, as λ1 and λ2 approach 0, it signifies that the parameter has no effect and the equation transforms into the least squares method, while moving towards infinity indicates that the parameter is increasing and regression coefficients will be almost equal to zero. For the training of the Elastic-Net regression, the optimal hyperparameters have been found as "λ1=0.355" and "λ2=0.331".

In the ML.Net application conducted through Microsoft Visual Studio 2022, the optimal model selected is "FastTreeRegressionTrainer" and the optimal hyperparameter values are shown in Table 3. Finally, for the OLS regression, the constant and variables coefficients of the mathematical function were found.

After determining the optimal parameters, regression models were created using the training dataset. Model validation was performed using the test dataset. Table 4 shows the R2, MAE, MSE, and RMSE over the Lasso, Elastic-Net, ML.Net and OLS regression models for the land value prediction.

Table 4. Optimal hyperparameters of the regression models

Performance metrics		R^2	MAE	MSE	RMSE
Lasso	Training	0.88	0.034	0.003	0.053
	Test	0.74	0.050	0.006	0.076
Elastic-Net	Training	0.89	0.031	0.003	0.051
	Test	0.79	0.043	0.004	0.065
ML.Net	Training	0.94	0.028	0.002	0.047
	Test	0.82	0.043	0.005	0.060
OLS	Training	0.84	0.039	0.004	0.060
	Test	0.73	0.052	0.007	0.081

Among various regression methods, it has been concluded that ML.Net (FastTreeRegressionTrainer) model yields superior results. The results of the Lasso and Elastic-Net models have shown similarity between training and test data. The success of these models is slightly higher compared to OLS regression (Table 4). In comparison to the most commonly used method in land valuation, which is OLS, the fact that ML.Net performs 9% better in terms of test data is highly significant within the scope of the study. This situation implies that ML.Net improves the prediction results by 9% compared to OLS in predicting land market values. The accordance between predicted values from regression models and the market value of the lands subject to sale has been assessed using test data (Figure 3).

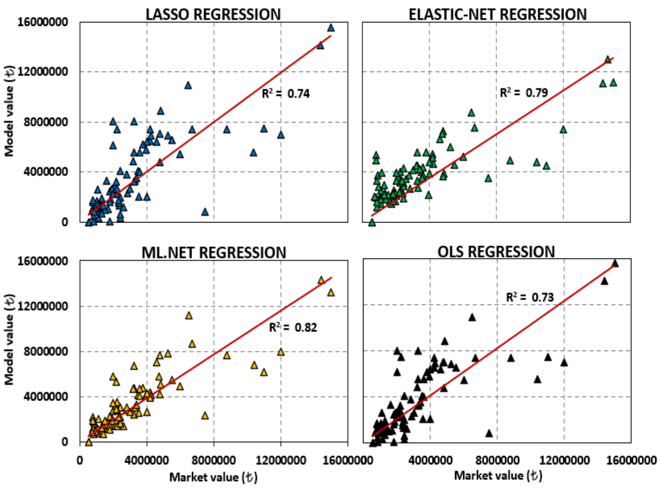

Figure 3. The accordance between model and market values (for test data)

Based on the graphical distributions in Figure 3, an R^2 value approaching 1 and data points nearing the trend line indicate that the model results are closer to market values. The R^2 between the predicted land values and market values are found to be 0.74, 0.79, 0.82, and 0.73 for Lasso, Elastic-Net, ML.Net, and OLS methods, respectively. From the results, it can be observed that Lasso and OLS regression produce similar outcomes, while Elastic-Net regression yields slightly different results compared to these two methods. Due to the similarity in the mathematical equations underlying Lasso and OLS models, there are no significant prediction differences.

Particularly, in modeling lands with high-market values within the dataset, the ML.Net algorithm has shown better performance and achieved good results compared to other methods. Therefore, for datasets with a small number of lands with high market values, ML.Net modeling can be recommended.

4. Conclusion

Valuation methods play a crucial role in accurately predicting and comprehending values in the real estate market. This study has examined the significance and impact of Lasso, Elastic-Net, ML.Net and OLS regression models in the field of land valuation. As a result of the ML.Net modeling, successful performance (test data) results were obtained with MAE=0.043, MSE=0.005, RMSE=0.060, and R2=0.82 metric values. Compared to OLS, which is frequently encountered in the literature when determining market value, the better performance of ML.Net (about 9%) is quite notable for this study. ML.Net provides users with a wide range of features, assisting in tasks ranging from data analysis for land valuation to predictions. Features such as fast model training, data preprocessing tools, multi-platform support, and integration of pre-trained models make ML.Net a strong choice for users predicting real estate values.

Author Contributions

Author1: Conceptualization, methodology, visualization, investigation. **Author2**: Data curation, writing-original draft preparation, writing-reviewing and editing

Statement of Conflicts of Interest

There is no conflict of interest between the authors.

Statement of Research and Publication Ethics

Research and publication ethics were complied with in the study.

References

Demetriou, D. (2016). The assessment of land valuation in land consolidation schemes: The need for a new land valuation framework. *Land use policy*, 54, 487-498. https://doi.org/10.1016/j.landusepol.2016.03.008

Derdouri, A., & Murayama, Y. (2020). A comparative study of land price estimation and mapping using regression kriging and machine learning algorithms across Fukushima prefecture, Japan. *Journal of Geographical Sciences*, 30, 794-822. https://doi.org/10.1007/s11442-020-1756-1

Dismuke, C., & Lindrooth, R. (2006). Ordinary least squares. *Methods and designs for outcomes research*, 93(1), 93-104.

Doan, Q. C. (2023). Determining the optimal land valuation model: A case study of Hanoi, Vietnam. *Land use policy*, 127, 106578. https://doi.org/10.1016/j.landusepol.2023.106578

Foryś, I., & Gaca, R. (2018). Intuitive methods versus analytical methods in real estate valuation: preferences of Polish real estate appraisers. *In Problems, Methods and Tools in Experimental and Behavioral Economics: Computational Methods in Experimental Economics (CMEE) 2017 Conference*. Łódź, Poland 79-87.

Hu, S., Yang, S., Li, W., Zhang, C., & Xu, F. (2016). Spatially non-stationary relationships between urban residential land price and impact factors in Wuhan city, China. *Applied Geography*, 68, 48-56. https://doi.org/10.1016/j.apgeog.2016.01.006

Kokot, S., & Gnat, S. (2019). Simulative verification of the possibility of using multiple regression models for real estate appraisal. *Real Estate Management and Valuation*, 27(3), 109-123. https://doi.org/10.2478/remav-2019-0029

Krause, A. L., & Bitter, C. (2012). Spatial econometrics, land values and sustainability: Trends in real estate valuation research. *Cities*, 29, 19S25. https://doi.org/10.1016/j.cities.2012.06.006

Microsoft. (2018). ML.Net: Machine Learning made for .Net. Microsoft.

Ramel, D. (2018). Open Source, Cross-Platform ML.Net Simplifies Machine Learning -- Visual Studio Magazine. *Visual Studio Magazine*.

Sisman, S. & Aydinoglu, A. C. (2022). Improving performance of mass real estate valuation through application of the dataset optimization and Spatially Constrained Multivariate Clustering Analysis. Land use policy, 119, 106167. https://doi.org/10.1016/j.landusepol.2022.106167

Sisman, S., Akar, A. U., & Yalpir, S. (2023). The novelty hybrid model development proposal for mass appraisal of real estates in sustainable land management. *Survey Review*, 55(388), 1-20. https://doi.org/10.1080/00396265.2021.1996797

Tibshirani, R. (1996). Regression shrinkage and selection via the lasso. *Journal of the Royal Stat. Society Series B: Statistical Methodology*, 58(1), 267-288. https://doi.org/10.1111/j.2517-6161.1996.tb02080.x

Zou, H., & Hastie, T. (2005). Regularization and variable selection via the elastic net. *Journal of the Royal Statistical Society Series B: Statistical Methodology*, 67(2), 301-320. https://doi.org/10.1111/j.1467-9868.2005.00503.x

Zurada, J., Levitan, A., & Guan, J. (2011). A comparison of regression and artificial intelligence methods in a mass appraisal context. *Journal of real estate research*, 33(3), 349-388. https://doi.org/10.1080/10835547.2011.12091311

Advanced GIS

http://publish.mersin.edu.tr/index.php/agis/index

e-ISSN:2822-7026

Land use and land cover classes affected by the possible sea level rise in Mersin city center (Türkiye)

Onur Güven*[1], Ümit Yıldırım[2], Cüneyt Güler[3], Mehmet Ali Kurt[4]

[1]*Bayburt University, Central Research Laboratory, Bayburt, Türkiye*
[2]*Bayburt University, Faculty of Applied Sciences, Department of Emergency Aid and Disaster Management, Bayburt, Türkiye*
[3]*Mersin University, Engineering Faculty, Department of Geological Engineering, Mersin, Türkiye*
[4]*Mersin University, Engineering Faculty, Department of Environmental Engineering, Mersin, Türkiye*

Keywords
Sea Level Rise,
Coastal Area,
Land Use Change,
GIS,
Mersin

Research Article
Received: 29/11/2023
Revised: 23/02/2024
Accepted: 25/02/2024
Published: 02/04/2024

Abstract

In this study, a sea level rise (SLR) investigation was carried out in an area representing the Mersin city center located in the south of Türkiye. The study area covers an area of *ca.* 385 km^2. Future projections provided by the Intergovernmental Panel on Climate Change (IPCC) were used for the SLR assessment. These projections are for the years 2100, 2200, 2300, 2400, and 2500 and the SLR for these periods are 0.83 m, 2.03 m, 3.59 m, 5.17 m, and 6.63 m, respectively. It is aimed to determine the areas affected by the SLR that will occur according to these projections. In this context, land use and land cover (LULC) data were obtained from the CORINE 2018 dataset. The data obtained were adapted within the boundaries of the study area and processesed using various GIS analyses. The results have shown that all LULC classes are greatly affected by the SLR, but in varying degrees. Land losses as a result of SLR are as follows: 0.4% at 0.83 m SLR, 9.8% at 2.03 m SLR, 16.7% at 3.59 m SLR, 21.6% at 5.17 m SLR, and 25% at 6.63 m SLR.

1. Introduction

Coastal regions are areas of critical importance in terms of the possible effects of climate change. Sea level rise (SLR) is one of the most important consequences of climate change affecting people living in coastal regions (Antonioli et al., 2020). It is inevitable that Türkiye, which is surrounded by the sea on three sides and has a coastline of 8,333 km (Demirkesen et al., 2008), will be affected by SLR. Türkiye's coasts are home to approximately 30 million people and produce more than half (~60%) of the country's gross production (Üstün, 2019). Sea water levels are rising due to two different parameters defined as the increasing water volume of the seas and their cumulative expansion (EPA, 2016).

The seawater level has increased by 98 mm from 1993 to the present (NASA, 2023) at a rate of 3.2 mm/yr over the last decades (Antonioli et al., 2020). The Mediterranean is one of the most vulnerable regions of the world to climate change, with 86% of the region's World Heritage sites at risk of water inundation and erosion (Reimann et al., 2018). According to data based on tide measurements, the SLR in the Mediterranean basin is 1.8 mm/yr (Antonioli et al., 2020).

City of Mersin borders the Taurus Mountains to the north, the Mediterranean Sea to the south, Antalya province to the west, and Adana province to the east. Mersin is a port city on the Mediterranean coast in southern Türkiye. Mersin is the city that has the longest coastline in Türkiye, with a length of *ca.* 321 km. The population of Mersin is 1,916,432 as of the end of 2022, and it is one of the most populous cities in Türkiye. In Mersin, the urban population continues to increase yearly. Mersin covers an area of 15,485 km^2, of which 53% consists of forests, 21% is agricultural lands, 22% is non-agricultural lands, and 4% is meadows and pastures (MTSO, 2023). Mersin's agricultural product diversity is high due to its suitable climatic conditions, flat areas with fertile soils brought by rivers, and its location on the coast (Kafalı Yılmaz, 2008). In addition, Mersin, which ranks first in Türkiye with a container business volume of 2.1 million TEU, has an essential economic infrastructure in maritime trade (MIP, 2021).

Many studies were conducted on the SLR in Türkiye, but studies on micro-scale areas are limited (Demirkesen et al., 2008; Geymen & Dirican, 2016; Kuleli et al., 2009; Kurt & Li, 2020; Simav et al., 2015; 2016; Üstün, 2019; Zengin, 2023). In this study, Mersin city center was chosen as the study area, which resides within the

***Corresponding Author**

*(onurguven@bayburt.edu.tr) ORCID 0000-0001-5608-7633
(umityildirim@bayburt.edu.tr) ORCID 0000-0002-7631-7245
(cguler@mersin.edu.tr) ORCID 0000-0001-8821-6532
(malikurt@mersin.edu.tr) ORCID 0000-0001-7255-2056

Cite this article

Güven, O., Yıldırım, Ü., Güler, C., & Kurt, M. A. (2024). Land use and land cover classes affected by the possible sea level rise in Mersin city center (Türkiye). *Advanced GIS,* 4(1), 15-23.

borders of three districts. In the present study, LULC types affected by SLR was evaluated using GIS technology and currently available climate projections.

2. Method

2.1. Study area

The study area (covering 385.4 km^2) constitutes the center of Mersin city, located on the Mediterranean coast in the south of Türkiye (Figure 1). While the study area is a narrow coastal plain in the west, it expands like a fan towards the east. Müftü Stream and Deliçay River are the important rivers of the study area. The climate in the study area is typically Mediterranean, characterized by hot and dry summers and relatively mild and rainy winters. The average annual rainfall is 613.2 mm, and the average annual temperature is 19.3 °C in the study area (MGM, 2023).

The population density of the Mersin city center is increasing every year due to constant migration. It is estimated that approximately 695,000 people live in this area. Transportation is provided by highways (O-51 and D400), railway (Adana-Mersin), and seaway. On the other hand, there is a marina and seaport (MIP) where international trade takes place. The internationally active and one of the largest industrial establishments in the region, the soda/chromium industry, is located on the east coast of the study area.

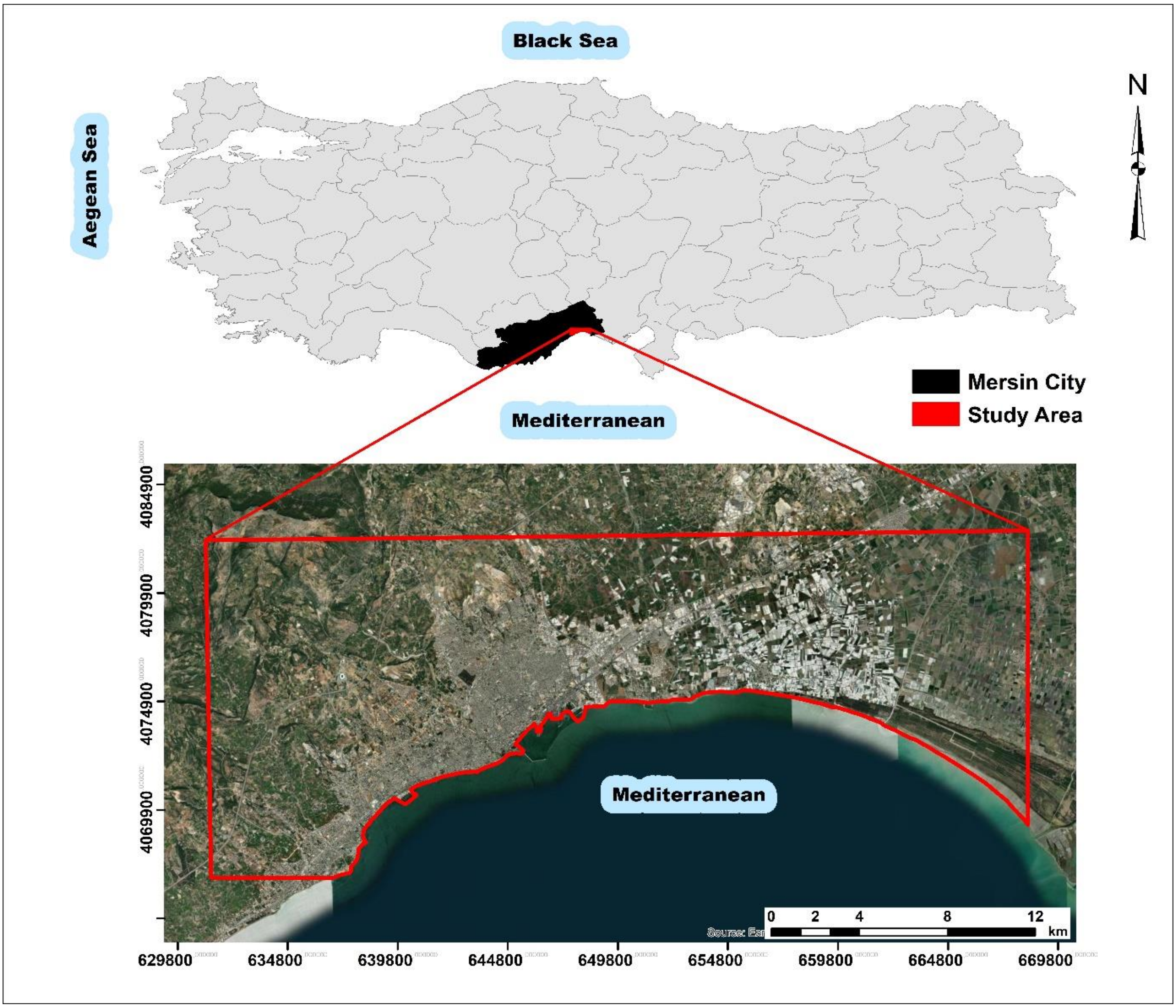

Figure 1. Map of the study area representing Mersin city center

The slope is an important parameter controlling many coastal regions' SLR effects over time (Al-Jeneid et al., 2008). The study area has a slope between 0°-65°. (Figure 2). Low-slope areas from west to east cover large areas. The slope of these areas is less than 10°.

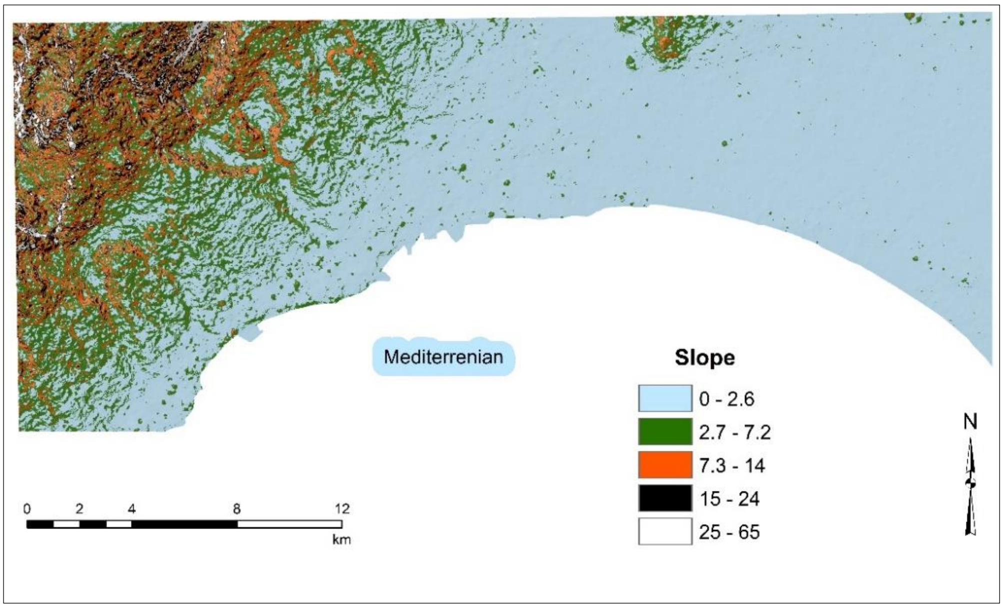

Figure 2. Slope map of the study area

2.2. Sea level rise

A digital elevation model (DEM) was used to determine the future areas of seawater inundation. Contour lines were taken as a basis when creating the DEM. DEM with a resolution of 10×10 m was obtained by digitizing 1:25,000-scale topographic maps (Figure 3) using ArcGIS 10.4 software (ESRI, 2016). All data used in this study were georeferenced using the WGS 1984 UTM Zone 36N coordinate system. The topographic elevations in the study area ranges from 0 m to 901 m. The distance of highland areas to the sea decreases towards the west.

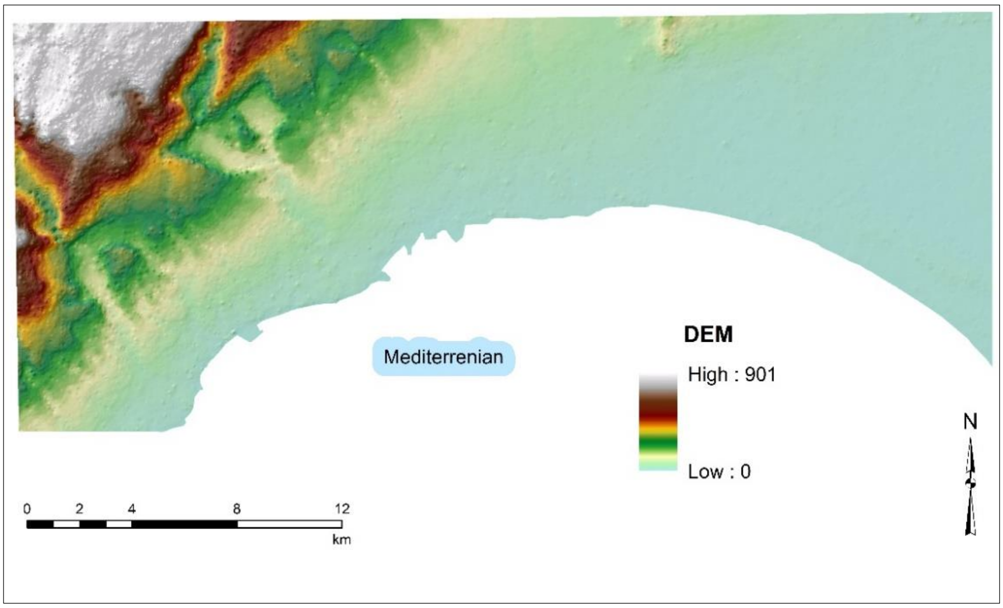

Figure 3. Digital elevation model (DEM) of the study area

The scenarios in the Intergovernmental Panel on Climate Change (IPCC) report (IPCC, 2014) revealed the risk situation due to SLR in the study area. The report includes SLR scenarios for the years 2100, 2200, 2300, 2400, and 2500. SLR scenarios are divided into three categories based on low, medium, and high CO_2 concentrations (IPCC, 2014). In this study, the SLR scenario applied according to high CO_2 concentration is taken as a reference, and SLR values are presented by the years in Table 1.

Table 1. IPCC 5th Assessment Report on SLR scenarios

Scenario (Year)	2100	2200	2300	2400	2500
SLR (m)	0.83	2.03	3.59	5.17	6.63

2.3. Land use and land cover

This study aims to determine the LULC classes affected by the SLR for Mersin city center. LULC data in grid format obtained from the CORINE dataset (EEA, 2018) was used to create the LULC layer for the study area. CORINE is a LULC dataset using satellite imagery and a computer-aided visual interpretation technique (Kaya & Demir, 2022).

LULC parameters (Figure 4) adapted to the study area are classified into 13 individual classes (Table 2).

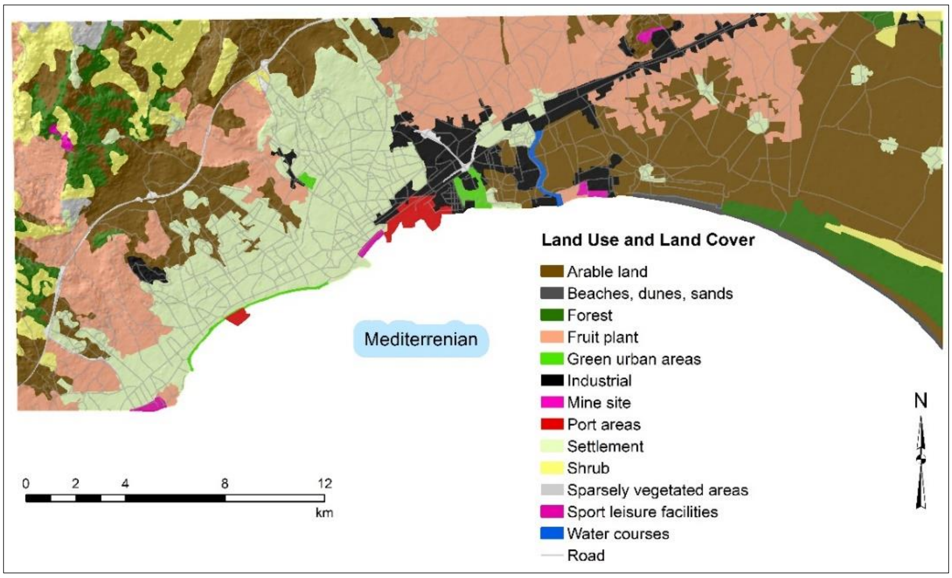

Figure 4. Map showing the LULC classes of the study area

Table 2. LULC types of the study area

LULC	Area (km²)	LULC	Area (km²)
Arable land	145.0	Sparsely vegetated areas	2.1
Fruit plants	89.0	Green urban areas	2.1
Settlement	72.9	Beaches, dunes, sands	2.1
Forest	23.2	Mine site	1.1
Industrial	22.6	Sport-leisure facilities	0.6
Shrub	21.6	Water courses	0.6
Port areas	2.5	**Total**	**385.4**

2.4. Data processing

The methodology followed to determine the inundation areas depending on the SLR and create spatial results is shown in the flow chart (Figure 5).

The Fill tool was used to remove sinks that may occur in the DEM data. Several calculations made use of this newly created DEM. Using Map Algebra in the raster calculator, sea level and SLR values given in Table 1 were calculated, respectively. The inundation areas were then determined by subtracting each SLR value from sea level, one at a time.

Where sea level inundation is anticipated, the sea level rise rasters have 1s; in other places, they have 0s or null values. As a result, the LULC where seawater inundation would occur was determined by multiplying this raster by the LULC raster. Finally, numerical results were obtained by calculating the number of pixels containing each land use value in square kilometers (km²).

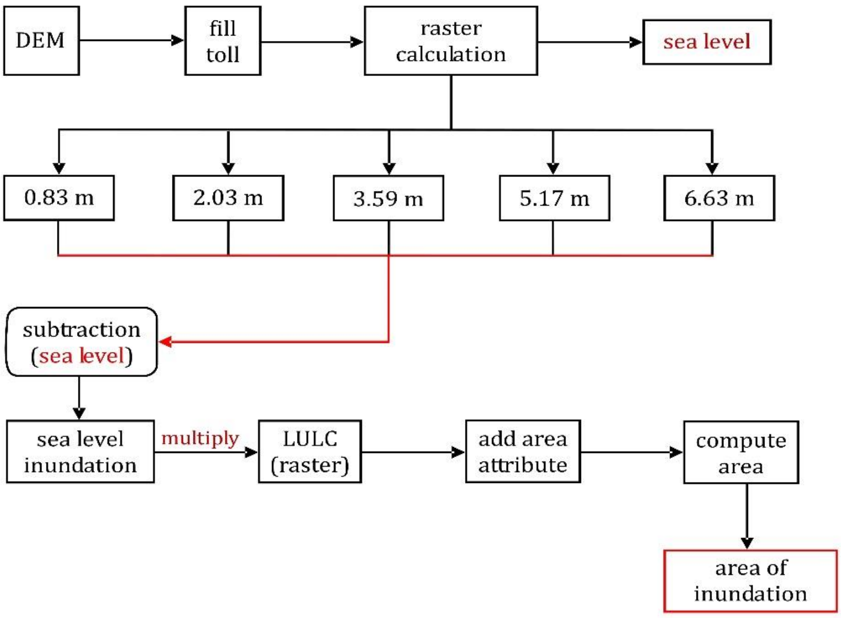

Figure 5. The flow chart depicting the methodology used in this study

3. Results

In this study, five different SLR scenarios (0.83 m, 2.03 m, 3.59 m, 5.17 m, and 6.63 m) were considered for the Mersin city center. The areas most affected by these scenarios are located at the east of the study area (Figure 6). This area is a coastal plain formed by alluvial deposits brought by the Deliçay and Tarsus rivers. This area's slope, characterized by a delta environment, varies between 0°-10°. In addition, the city's important agricultural areas are located in the most sensitive area with respect to SLR.

LULC types affected by the combination of SLR and LULC were determined spatially (Table 3 and Figure 12). Except for sparsely vegetated areas, all LULC classes were affected by different SLR scenarios. The most affected classes were arable land and forest. A section of the Adana-Mersin highway (D400) is inundated when sea level rise by 6.63 m. LULC losses in SLR scenarios for 2100, 2200, 2300, and 2500 are 0.4%, 9.8%, 16.7%, 21.6%, and 25.0%, respectively.

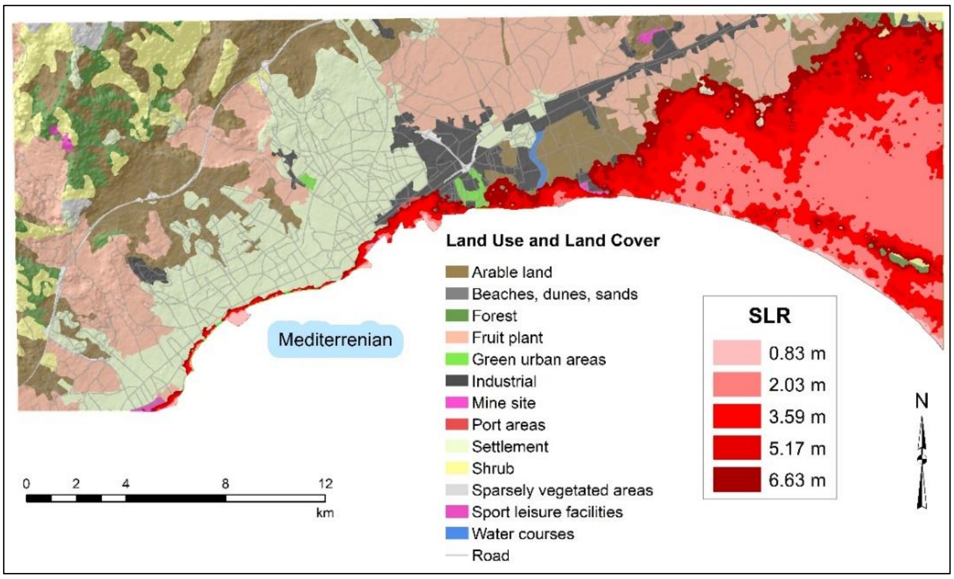

Figure 6. Sea level rise (SLR) map of the study area for the five IPCC scenarios

At 0.83 m SLR, the affected area is minimal (Figure 7). The most affected LULC type was beaches, dunes, and sands, followed by the port area. The loss of this area is 33%. Roads will not be affected by the sea water inundation. Approximately, 0.4% of the total area was inundated by the sea in 2100.

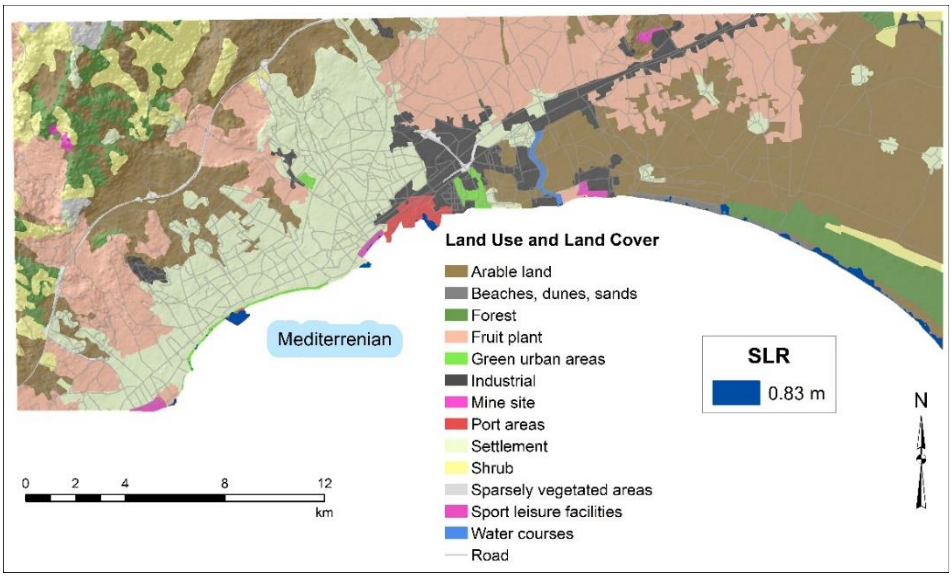

Figure 7. Sea level rise (SLR) map of 0.83 m SLR (year 2100)

However, by the year 2200, 9.8% of the total area will be inundated by the sea (Figure 8). LULC-type named arable lands are most affected (30.8 km^2) by 2.03 m SLR. According to the results, 76% of the beaches, dunes, and sands will be inundated by the year 2200. Forests have the most land loss after arable land. Some roads east of the study area will be affected by 2.03 m SLR. Industrial, shrub, and mine site LULC classes also will be affected by the SLR.

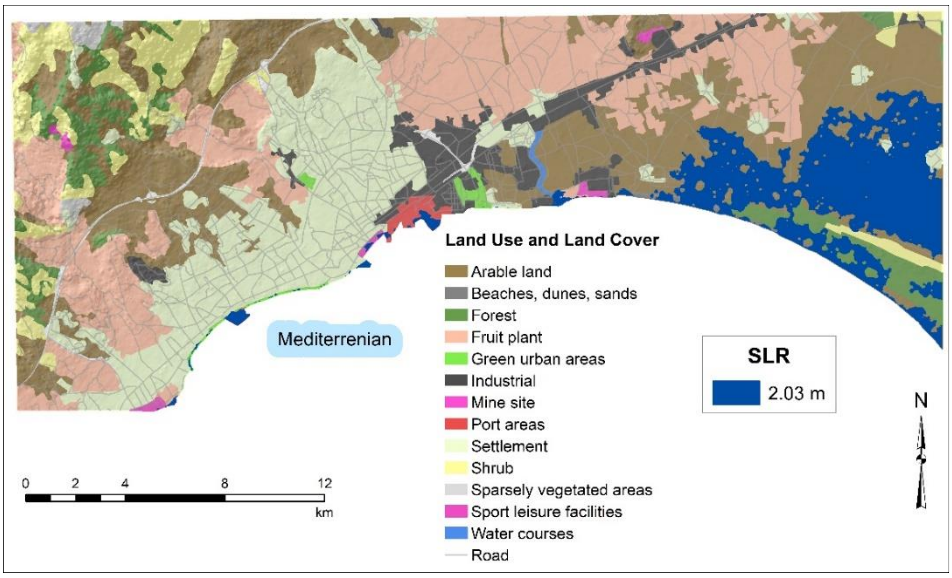

Figure 8. Sea level rise (SLR) map of 2.03 m SLR (year 2200)

A 3.59 m rise in sea level will led to the loss of one-third of arable land. 16.7% of the total area will be inundated by the sea (Figure 9). Significant economic losses will likely occur in the port area, more than half of which is inundated. Most of the forests in the coastal zone were affected by the 3.59 m SLR. With this rise, part of the coastal roads will be affected by the SLR.

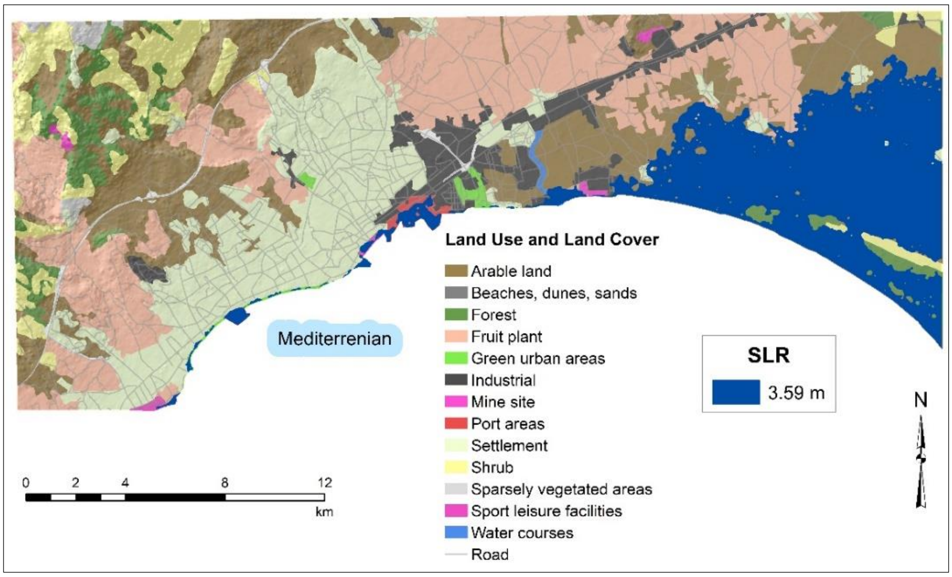

Figure 9. Sea level rise (SLR) map of 3.59 m SLR (year 2300)

At 5.17 m SLR, beaches, dunes, and sands will be completely inundated. Half of the sports-leisure facilities were also inundated. According to this scenario, 21.6% of the total area will be inundated by the year 2400 (Figure 10). Depending on the elevation and slope, there is a considerable land loss in the east of the study area. In this area, most of the forests, along with arable land, will be occupied by the seawater.

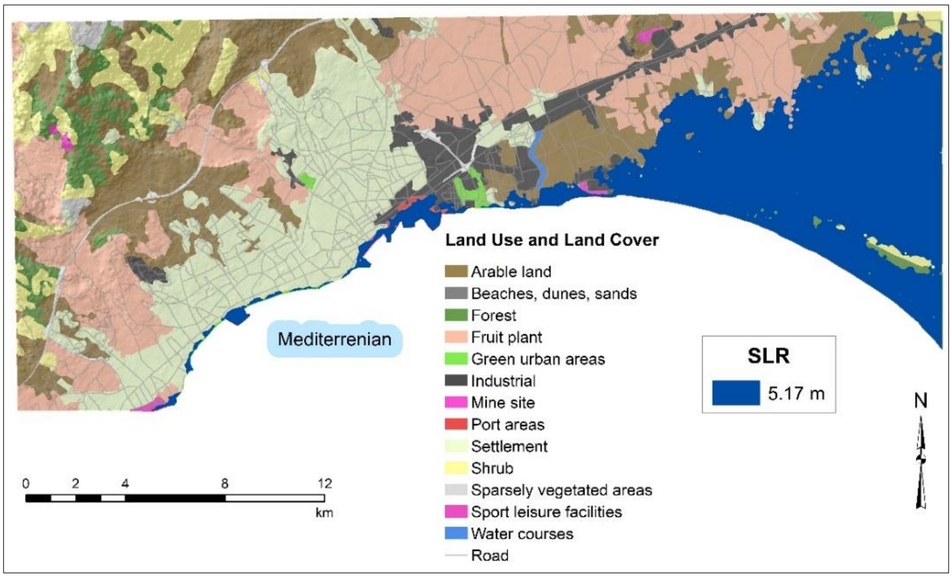

Figure 10. Sea level rise (SLR) map of 5.17 m SLR (year 2400)

IPCC's year 2500 scenario of 6.63 m SLR has the most significant impact. According to this scenario, 21.6% of the total area will be inundated by the sea (Figure 11). Nearly, 92% of the port area is affected by the SLR. The loss of arable land is 68.1 km². The forest area in the coastal region is about to disappear. At the same time, most of the agricultural areas east of the study area, namely the Tarsus Plain, will be inundated. As a result of this rise, a part of the intercity highway, as well as the coastal road will also be inundated.

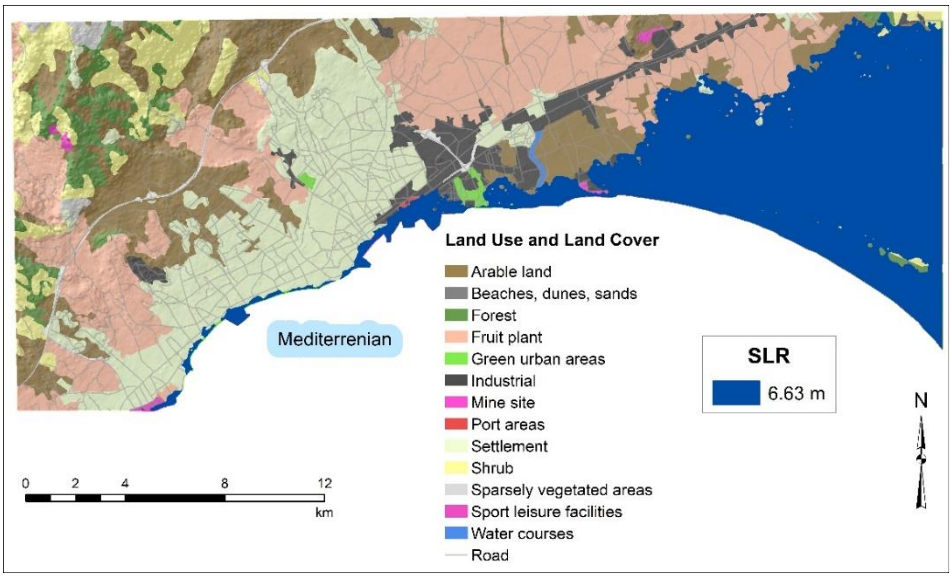

Figure 11. Sea level rise (SLR) map of 6.63 m SLR (year 2500)

Table 3. LULC classes affected according to different SLR scenarios

	SLR Scenarios				
	0.83 m (2100)	2.03 m (2200)	3.59 m (2300)	5.17 m (2400)	6.63 m (2500)
LULC	LULC Loss (km²)				
Arable land	0.3	30.8	49.2	61.3	68.1
Fruit plants	0.03	0.2	1.2	2.8	4.6
Settlement	0.07	0.3	1.1	2.4	3.6
Forest	0.09	3.8	7.8	9.4	10.2
Industrial	-	0.1	0.3	1.1	2.2
Shrub	-	0.02	0.2	1.0	1.7
Port areas	0.5	0.7	1.6	2.0	2.3
Sparsely vegetated areas	-	-	-	-	-
Green urban areas	0.03	0.1	0.4	0.5	0.7
Beaches, dunes, sands	0.7	1.6	2.0	2.1	2.1
Mine site	-	0.005	0.1	0.1	0.2
Sport-leisure facilities	0.02	0.1	0.2	0.3	0.4
Watercourses	0.01	0.1	0.1	0.1	0.2

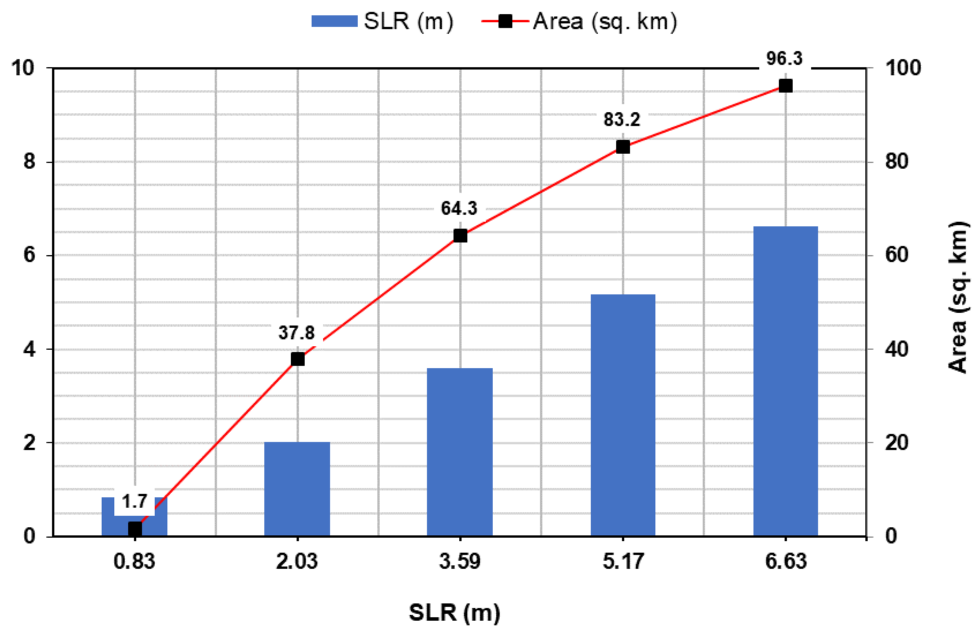

Figure 12. Total area (km^2) lost to sea level rise

4. Discussion

The Mersin city center, home to various LULC classes, was selected for the evaluation of the SLR effect. In addition, this city plays an important role in international trade.

Many studies conducted in Türkiye are large-scale studies covering all coastal provinces. According to Demirkesen et al. (2008), which identifies coastal areas being vulnerable to rising sea levels, some areas of Mersin are at high risk. Similar results were also obtained in the study of Kuleli et al. (2009). The eastern region of our study area (Adana provincial border) is one of the most vulnerable regions of Türkiye to SLR. The studies conducted by the other researchers also support this study.

This study can be considered as a micro-scale when considered on a country basis. Studying smaller areas is essential in terms of climate change and water management. In this study, only global scenarios presented by IPCC are considered.

The delta regions of the study area are in great danger due to rising sea levels. Economic activities here will be interrupted in the future due to SLR. These results reveal the fact that in the future SLR will have important socio-economic and ecological effects. In addition to socio-economic and ecological impacts, the impact of rising sea levels on historical and archaeological sites is significant. The results of this situation can be found in a study conducted by Zengin (2023). Soli Pompeipolis Ancient Port in Mersin is at very high risk for SLR.

Micro-scale studies can raise awareness for policymakers and local governments. The outputs of such studies can be used as a base for studies such as sustainable water management, coasts, and catchments. With SLR, not only land loss but also population migration is inevitable. Therefore, branches of science such as climate change, economics, sociology, and ecology should be considered together to find a solution to this important global problem.

5. Conclusion

To evaluate the SLR effect, the study area within the borders of Mersin city center, covering three districts was selected. 10×10 m resolution DEM data served as the basis for the SLR investigation. Contour lines were used to produce the DEM. CORINE 2018 LULC dataset was adapted to the study area to evaluate LULC types affected by SLR. A total of 13 LULC classes were defined in the study area. These LULC classes were combined with the SLR, and the affected areas were calculated.

According to data collected, arable land was the most impacted LULC class (at 6.63 m SLR). It was followed by forests, fruit plants, settlements, port areas, industrial, beaches-dunes-sands, shrubs, green urban areas, sports-leisure facilities, mine sites, water courses LULC types. Land losses as a result of SLR are as follows: 0.4% at 0.83 m SLR, 9.8% at 2.03 m SLR, 16.7% at 3.59 m SLR, 21.6% at 5.17 m SLR, and 25% at 6.63 m SLR.

Acknowledgement

This study was presented as an oral presentation at Intercontinental Geoinformation Days (IGD) 2023 and published in full text in the proceedings book.

Author Contributions

Onur Güven: Writing draft, methodology, software. **Ümit Yıldırım**: Visualization, data curation, writing draft. **Cüneyt Güler**: Writing, investigation, reviewing. **Mehmet Ali Kurt:** Investigation, writing, reviewing.

Statement of Conflicts of Interest

There is no conflict of interest between the authors.

Statement of Research and Publication Ethics

Research and publication ethics were complied with in the study.

References

Al-Jeneid, S., Bahnassy, M., Nasr, S., & El Raey, M. (2008). Vulnerability assessment and adaptation to the impacts of sea level rise on the Kingdom of Bahrain. *Mitig Adapt Strat Glob Change*, 13(1), 87–104. https://doi.org/10.1007/s11027-007-9083-8

Antonioli, F., De Falco, G., Lo Presti, V., Moretti, L., Scardino, G., Anzidei, M., Bonaldo, D., Carniel, S., Leoni, G., Furlani, S., MArsico, A., Petitta, M., Randazzo, G., Sc,cchitano, G., & Mastronuzzi, G. (2020). Relative sea-level rise and potential submersion risk for 2100 on 16 coastal plains of the Mediterranean Sea. *Water*, 12(8), 2173. https://doi.org/10.3390/w12082173

Demirkesen, A. C., Evrendilek, F., & Berberoğlu, S. (2008). Quantifying coastal inundation vulnerability of Turkey to sea-level rise. *Environmental Monitoring and Assessment*, 138(1-3), 101-106. https://doi.org/10.1007/s10661-007-9746-7

EEA. (2018). *CORINE land cover 2018 (vector/raster 100 m), Europe, 6-yearly*. Retrieved October 22, 2023 from https://land.copernicus.eu/pan-european/corine-land-cover/clc2018?tab=download

EPA. (2016). *Climate change indicators in the United States.* Fourth edition. https://www.epa.gov/sites/default/files/2016-08/documents/climate_indicators_2016.pdf

ESRI (2016). *ArcGIS 10.4.1 and ArcGIS Pro 1.3 corporate distribution*. Esri.

Geymen, A., & Dirican, A. Y. (2016). Analysis sea level change due to climate change using Geographical Information Systems. *Electronic Journal of Map Technologies,* 8(1), 65-74. https://doi.org/10.15659/hartek.16.04.308

IPCC. (2014). *Climate change 2014: Synthesis report*. Geneva, Switzerland.

Kafalı Yılmaz, F. (2008). *Adana Ovaları'nda iklim-tarım ilişkisi ve tarım politikalarının yansıması*. A.K.Ü. Yayınları.

Kaya, H. E., & Demir, V. (2022). Estimation of land use and land cover changes in Konya closed basin. *Proceedings Book of the 4th Intercontinental Geoinformation Days,* Tabriz, Iran, 180-183.

Kuleli, T., Şenkal, O., & Erdem, M. (2009). National assessment of sea level rise using topographic and census data for Turkish coastal zone. *Environmental Monitoring and Assessment*, 156(1-4), 425-434. https://doi.org/10.1007/s10661-008-0495-z

Kurt, S., & Li, X. (2020). Potential impacts of sea level rise on the coasts of Turkey. *Journal of Environment and Earth Science*, 10(5), 40–47. https://doi.org/10.7176/JEES/10-5-04

MGM. (2023). *Resmi istatistikler (n Turkish)*. Retrieved October 26, 2023, from https://www.mgm.gov.tr/veridegerlendirme/il-ve-ilceler-istatistik.aspx?m=MERSIN

MIP. (2021). *Mersin uluslararasi limani sürdürülebilirlik raporu (in Turkish).* Retrieved October 22, 2023 from https://www.mersinport.com.tr/tr/Images/ContentImages/Mip_2021_Surdurulebilirlik_Raporu.pdf

MTSO. (2023). *2022 Mersin ekonomik raporu* (in Turkish). https://www.mtso.org.tr/tr/a/2022-mersin-ekonomik-raporu

NASA. (2023). Sea *level*. Retrieved October 11, 2023, from https://climate.nasa.gov/vital-signs/sea-level/

Reimann, L., Vafeidis, A. T., Brown, S., Hinkel, J., & Tol, R. S. J. (2018). Mediterranean UNESCO World Heritage is at risk from coastal flooding and erosion due to rising sea levels. *Nature Communications*, 9, 4161. https://doi.org/10.1038/s41467-018-06645-9

Simav, Ö., Şeker, D. Z., Tanık, A., & Gazioğlu, C. (2015). Determining the endangered fields of Turkish coasts with coastal vulnerability index. *Harita Dergisi*, 153(81), 1-8.

Üstün, Y. M. (2019). Possible effects of sea level change due to anthropogenic climate change on Sinop peninsulai. *Journal of Disaster and Risk*, 2(2), 64-79. https://doi.org/10.35341/afet.567218

Zengin, E. (2023). Inundation risk assessment of Eastern Mediterranean Coastal archaeological and historical sites of Türkiye and Greece. *Environmental Monitoring and Assessment*, 195(8), 1–25. https://doi.org/10.1007/s10661-023-11549-3

Advanced GIS
http://publish.mersin.edu.tr/index.php/agis/index
e-ISSN:2822-7026

A geo-spatial analysis of precipitation distribution and its impacts on vegetation in Rwanda

Rosette Ambiance Shema*[1,2,3,4], Li Lanhai[1,2,3,4]

[1]Xinjiang Institute of Ecology and Geography (XIEG), Chinese Academy of Sciences (UCAS), Urumqi, China
[2]University of Chinese Academy of Sciences (UCAS), China
[3]Xinjiang Key Laboratory of Water Cycle and Utilization in Arid Zone, Urumqi, China
[4]Research Center for Ecology and Environment of Central Asia, Chinese Academy of Sciences, Urumqi, China

Keywords
GIS,
Spatial Analysis,
Remote Sensing,
Precipitation,
Vegetation Cover

Research / Review Article
Received: 04/12/2023
Revised: 17/02/2024
Accepted: 19/03/2024
Published: 02/04/2024

Abstract
Rwanda is home to a diverse and picturesque landscape that encompasses a range of ecosystems, including rainforests, savannas, and agricultural regions. The intricate relationship between rainfall patterns and vegetation types shapes these varied landscapes, which are crucial for supporting biodiversity and agricultural productivity across the country. Our comprehensive geospatial analysis employs advanced geographical information systems (GIS) techniques and remote sensing data to assess spatial and temporal variations in precipitation across distinct regions of the country. Utilizing historical precipitation data and satellite-derived vegetation indices, our analysis spans extensive periods, incorporating annual and monthly rainfall records from 1990 to 2020 and MODIS/Terra Vegetation Indices spanning 2000 to 2020. Advanced remote sensing methodologies are employed to investigate the correlations between precipitation patterns and vegetation dynamics. The study reveals discernible spatial variations in Rwanda's precipitation distribution, elucidating marked seasonal fluctuations. Identified regions experiencing notable changes in precipitation levels exhibit a direct impact on vegetation health and density. Recorded annual rainfall data illustrates variations across different years, indicating fluctuating levels such as 1160.1 mm (1990), 1078.2 mm (2000), 1402.4 mm (2010), and 1391.1 mm (2020). Corroborating NDVI imagery demonstrates increased vegetation cover in 2010 and 2020, aligning with higher recorded rainfall during these years. The research underscores the significance of these findings in understanding the intricate interplay between precipitation distribution and vegetation dynamics and offers actionable insights essential for sustainable land management, optimized resource allocation, and the formulation of resilience-building strategies. These insights are particularly crucial in the context of adapting to and mitigating the effects of climate change.

1. Introduction

Rainfall is a critical determinant of vegetation distribution globally, with high precipitation levels often characterizing dense forests and lower rainfall areas featuring grasslands, deserts, and arid landscapes (Kalisa et al., 2019; Shaw et al., 2023). Adequate rainfall is crucial for plant growth and photosynthesis, enabling vegetation to thrive. Precipitation patterns are vital for regulating ecosystem functions such as nutrient cycling, soil moisture, and hydrological processes. Changes in rainfall can significantly impact these functions, leading to potential adverse effects on the health and stability of ecosystems globally. Therefore, it is essential to monitor and comprehend precipitation patterns and their potential changes to safeguard the environment and promote sustainable development (Kirchmeier-Young & Zhang, 2020).

Rainfall patterns play a crucial role in shaping the diverse ecosystems of Africa, which include various biomes such as tropical rainforests, savannas, and deserts. The precipitation levels exert a direct influence on these biomes, with rainfall variation being a significant determinant of their distribution. Regions with sufficient precipitation are conducive to thriving lush rainforests, while arid and semi-arid areas sustain savannas or deserts due to limited rainfall (Mountjoy & Embleton, 2023). Beyond shaping the continent's ecosystems, rainfall plays a critical role in supporting agricultural activities across Africa. Seasonal rainfall patterns dictate planting and harvest cycles, and farmers rely heavily on these patterns for successful crop yields. However, changes in rainfall patterns, especially prolonged droughts or erratic rainfall, have significant implications for food security, livelihoods, and the overall well-being of communities reliant on agriculture (Algur et al., 2021; Shahzad et al., 2019).

***Corresponding Author**
*(ambiancerosette@outlook.com) ORCID 0009-0009-8640-4092
(lilh@ms.xjb.ac.cn) ORCID 0000-0002-8887-0531

Cite this article
Shema, R. A., & Lanhai, L. (2024). A geo-spatial analysis of precipitation distribution and its impacts on vegetation in Rwanda. *Advanced GIS,* 4(1), 24-30.

Rwanda, located in the central region of East Africa, boasts an impressive range of landscapes that owe their distinctiveness to the complex interplay between precipitation patterns and their profound effects on vegetation (de Dieu Ndayisenga & Mupenzi, 2020; Kuradusenge et al., 2021; Siebert et al., 2019). This small, landlocked country is blessed with a remarkable geographical mosaic and varied topography, which results in a tapestry of climatic zones that give rise to a diverse array of ecosystems. From the lush expanses of dense rainforests to the vast stretches of grassy savannas, Rwanda's topographical diversity creates an environment that nurtures a multitude of habitats, each uniquely shaped by the prevailing rainfall patterns. The rich variation in vegetation cover is intricately intertwined with the distribution of rainfall across the country, exerting a powerful influence not only on Rwanda's ecological richness and biodiversity but also on its socio-economic landscape. Agriculture is the cornerstone of Rwanda's economy, and the interdependence between rainfall and vegetation profoundly influences agricultural practices, determining planting seasons, crop choices, and overall productivity (de Dieu Ndayisenga & Mupenzi, 2020; Maue, 2021; Siebert et al., 2019). As such, the fluctuations in rainfall and resulting alterations in vegetation significantly shape the socio-economic fabric of the nation, affecting livelihoods, food security, and the overall well-being of its populace.

Hence, comprehending the crucial interplay between precipitation distribution and vegetation dynamics in Rwanda holds significant importance. Mainly, Rwanda's ecosystems are home to a wealth of biodiversity that requires meticulous conservation efforts, necessitating a detailed analysis of how these ecosystems respond to changing rainfall dynamics (Gatwaza & Wang, 2021; Maue, 2021). This study is an extensive geospatial investigation that utilizes advanced technology such as GIS and remote sensing data to examine the patterns of precipitation distribution across various regions of Rwanda. Additionally, this analysis aims to clarify the consequential impacts of these precipitation patterns on the vegetative cover, delineating how differing rainfall regimes influence the composition, health, and resilience of vegetation in different ecological zones. By delving into the intricacies of precipitation-vegetation relationships, this research not only contributes to the scientific understanding of Rwanda's ecosystem dynamics but also aims to provide actionable insights. These insights will inform targeted strategies for sustainable land management, resource allocation, and ecosystem preservation, ultimately enhancing Rwanda's resilience to the challenges posed by a changing climate.

2. Method

2.1. Description of the Study Area

Rwanda has five administrative provinces and 30 districts (Figure 1). Rwanda, a landlocked country located in East-Central Africa, is situated between latitudes 1.4484° S and 2.6842° S and longitudes 29.2842° E and 30.7413° E (Figure 2). It shares borders with Uganda to the north, Tanzania to the east, Burundi to the south, and the Democratic Republic of Congo to the west. Rwanda is known for its varied topography, including rolling hills, lush valleys, and numerous lakes, with its capital city, Kigali, positioned in the central part of the country. As of my last knowledge update in the last population census in 2022, Rwanda had an estimated population of around 13.2 million people, making it one of Africa's most densely populated nations (NISR, 2023).

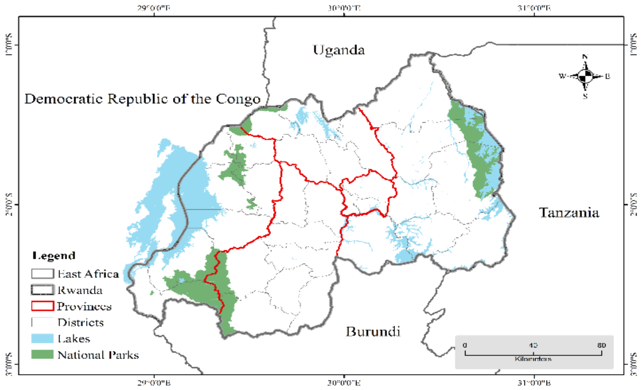

Figure 1. Administrative map of Rwanda

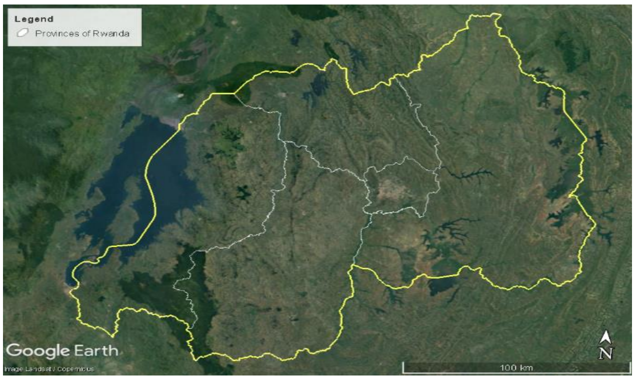

Figure 2. Google Earth Image of Rwanda

2.2. Topography

Rwanda is a stunning country located in Central/Eastern Africa, situated on a raised terrain that elevates approximately 1,200 meters above sea level. This beautiful country is characterized by its hilly topography with the majestic Virunga Mountains being the highest points. These mountains are located on the border with the Democratic Republic of the Congo, making for a breathtaking view. Standing tall at 4,507 meters, Mount Karisimbi is the highest mountain in Rwanda. Interestingly, the highest point in Rwanda is situated in the north, while the lowest is located in the west. It is worth noting that Rwanda's elevation ranges between 4507 and 900 meters above sea level, as depicted by Figure 3 and its mathematical results.

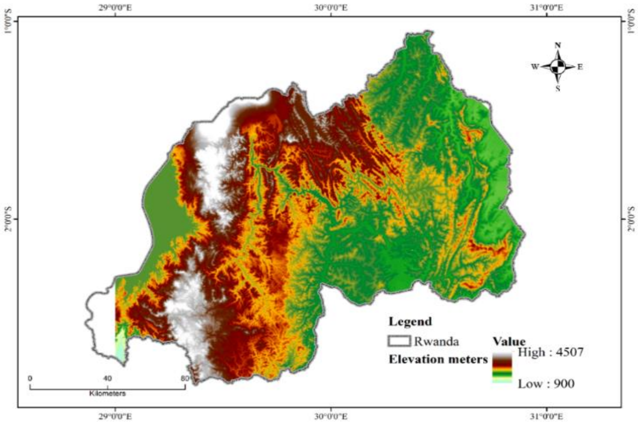

Figure 3. Topographic map of Rwanda

2.3. Data set

2.3.1. Data source

The primary focus of this investigation revolved around the detection of the normalized difference vegetation index (NDVI), a crucial indicator of vegetation health and distribution. The study area's vegetation dynamics were analyzed using MODIS-NDVI data, which had a resolution of 250 meters and were derived from MOD13Q1 (Table 2). The NASA Land Processes Distributed Active Archive Center provided the MOD13Q1 Terra vegetation index data from 2000 to 2020. Furthermore, Precipitation data from 1990 to 2020 were meticulously collected from the WorldClim web platform (Table 1). Due to the high prevalence of cloud cover in Landsat images, we transitioned to using MODIS NDVI data, which are available starting from the year 2000. As a result, we refrained from correlating rainfall data with NDVI prior to this year.

This supplementary information enriched the analysis by providing insights into how climatic factors may have influenced the observed changes in NDVI. To enhance the spatial context of the research, shapefiles and DEM were downloaded from two sources: DIVA-GIS and the Rwanda Spatial Data Hub (RSDH). These datasets, encompassing a broad spectrum of geographical attributes, bolstered the analytical rigor and facilitated a holistic perspective on the factors influencing the observed changes. Moreover, to ensure the accuracy and reliability of the gathered data, an additional layer of meteorological information was obtained directly from Mateo-Rwanda. This direct collaboration with local meteorological authorities validated the findings and improved the outcomes' precision.

Table 1. Data type and source

Data owner	Data type	Link
NASA	MODIS/Terra Vegetation Indices 16-Day L3 Global 250m (2000, 2010, & 2020)	https://ladsweb.modaps.eosdis.nasa.gov/
WorldClim	Monthly total precipitation (mm) with 10 minutes (~340 km^2) resolution (1990, 2000, 2010, & 2020)	https://worldclim.org/data/monthlywth.html
Government of Rwanda & DIVA-GIS	Spatial data: Boundary and DEM	https://www.diva-gis.org/gdata https://geodata.rw/portal/apps/sites/#/nsdi
METEO-Rwanda	Monthly Rainfall and Temperature data	https://meteorwanda.gov.rw/index.php?id=2

Table 2. MODIS/Terra vegetation indices

Year	Resolution	Date	Name
2000	250m	25/06/2000	MOD13Q1.A2000177.h21v09.061.2020048031344.hdf MOD13Q1.A2000177.h20v09.061.2020048031104.hdf
2010	250m	26/06/2010	MOD13Q1.A2010177.h20v09.061.2021168170801.hdf MOD13Q1.A2010177.h21v09.061.2021168180554.hdf
2022	250m	11/07/2020	MOD13Q1.A2020193.h21v09.061.2020340134419.hdf MOD13Q1.A2020193.h20v09.061.2020340134512.hdf

2.3.2. Data processing

2.3.2.1. Normalized difference vegetation index

NDVI is a widely utilized metric for assessing the vitality and density of plant cover through the analysis of light reflection across distinct spectral ranges. Its values are derived by analyzing the spectral data acquired by satellite sensors like Landsat, which capture information across various electromagnetic spectrum bands. The calculation of NDVI for each image followed a prescribed equation (Dehling & Sinsch, 2023). Typically, NDVI is computed utilizing a specific formula (Equation 1). However, our research employed NDVI data with a resolution of 250 meters. The ArcGIS project tool (Geoprocessing tool that projects spatial data from one coordinate system to another) combined and adjusted the NDVI data for 16-day composites (Yuan et al., 2019). The mosaics for each 16-day composite were transformed from a sinusoidal projection to ITRF_2005, a widely adopted projection in Rwanda. Finally, on each day, two images were downloaded, one for 35 and 36. Mosaic to New Raster tool (Geoprocessing tool that mosaics multiple raster datasets into a new raster dataset) was used to merge two images for each year, and Extract By Mask (Geoprocessing tool that extracts the cells of a raster corresponding to the area defined by a mask) was used to extract only NDVI map of Rwanda.

Raster Calculator and Image*0.0001 formula were used to put an image in the range between -1 to 1 values.

$$Landsat\ NDVI = (NIR - RED)/(NIR + RED) \quad (1)$$

where NIR is near-infrared reflectance, and RED is red reflectance.

NDVI values start from -1 to +1, with elevated positive values signifying robust and more densely vegetated areas. Furthermore, researchers used average annual and monthly rainfall data in this article. This helped us to create Excel graphs illustrating how monthly rainfall changes. These graphs make it simple to spot any patterns or connections between agriculture and rainfall.

2.3.2.2. Annually and monthly rainfall

The study conducted a comprehensive analysis of the influence of rainfall on agriculture in Rwanda using annual and monthly rainfall data spanning from 1990 to 2020 (Figure 4). The data was acquired from the WorldClim website and was accurately processed to integrate with ArcGIS 10.8.2. To ensure accuracy, 320 weather stations situated across Rwanda were utilized as sampling points within the Spatial Analyst tool. In addition to the global climate data, the localized information was also incorporated into the analysis to produce a detailed and accurate assessment of climate change patterns in the region. The Inverse Distance Weighting (IDW) interpolation method was applied to extrapolate data points, facilitating the creation of continuous raster layers that depict rainfall's spatial and temporal trends.

The study's integrated approach combines global climate data with locally collected information to provide a comprehensive understanding of climate change patterns in the region. By using a combination of global and local data, the study provides a detailed and accurate assessment of the impact of rainfall on agriculture in Rwanda. This information is critical to better-informed decision-making and mitigation efforts aimed at addressing the challenges posed by climate variability and change.

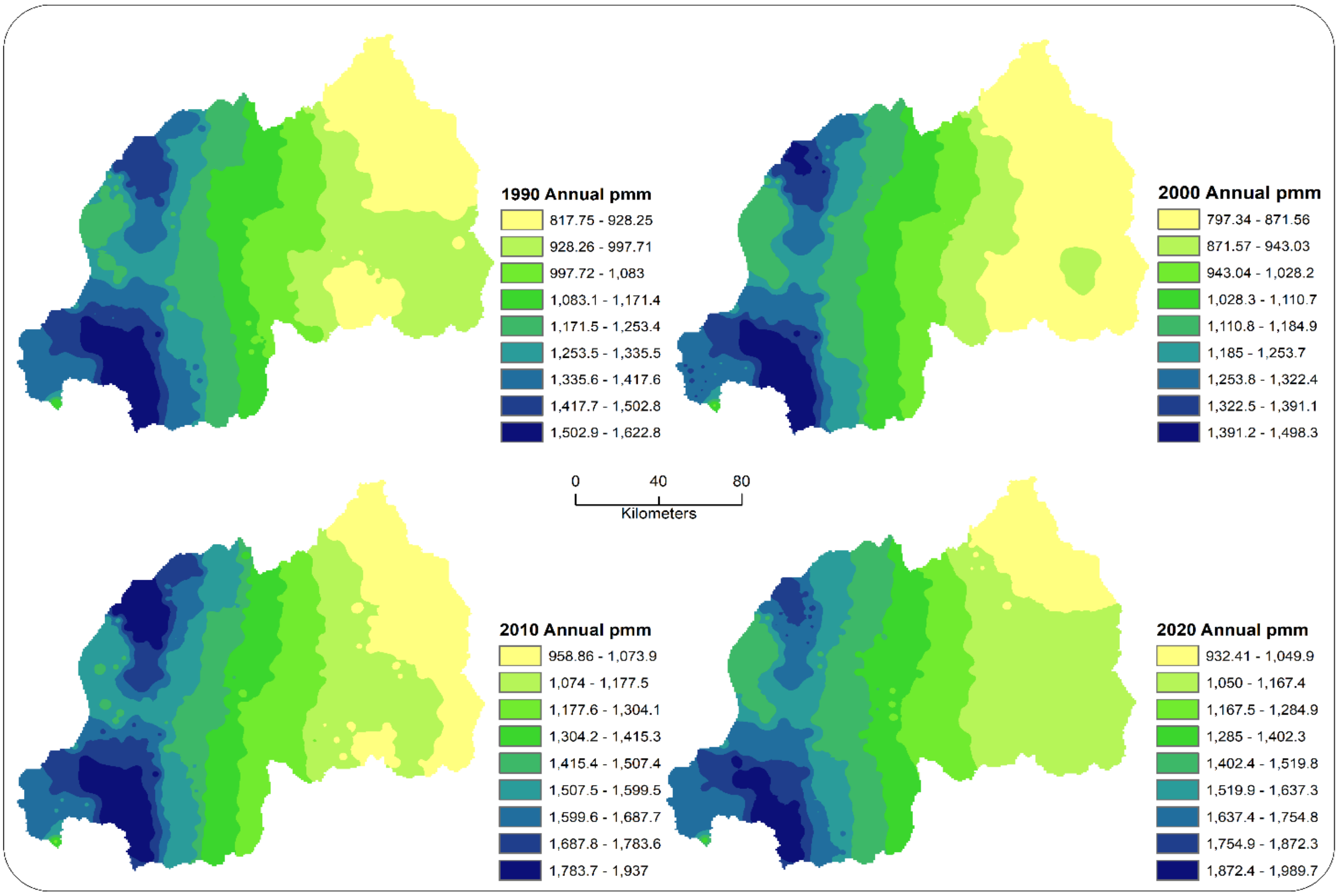

Figure 4: Rainfall change from 1990 to 2020

3. Results and discussion

3.1. Rainfall variability and vulnerability

The significance of precipitation as a climatic factor for agriculture cannot be overstated, and with climate change, precipitation patterns are changing globally. In some regions, precipitation is becoming less frequent but more intense; in others, it is becoming more variable and unpredictable. These changes considerably impact crop yields, water availability, and pest and disease pressure. Figure 4 illustrates alterations in rainfall patterns across various years, highlighting spatial variations. The eastern part of Rwanda consistently experiences a rainfall shortage, adversely affecting neighboring provinces. On a nationwide scale, in 1990, precipitation levels ranged from 817.75 to 1,622.8 mm, while in 2000, they varied between 797.34 and 1,498.3 mm. In 2010, rainfall spanned from 958.86 to 1,937 mm; in 2020, it ranged from 932.41 to 1,989.7 mm.

Figure 4 shows that the rainfall distribution in Rwanda varies from east to west, with the western regions receiving more rainfall than the eastern regions. This is due to the country's topography, with the western regions being higher in elevation and receiving more precipitation from the Congo Basin. The rainfall also varies yearly, with some years being wetter than others.

Maps-based analysis shows that the country's western regions consistently receive more rainfall than the eastern regions. In all four years, the annual rainfall in the western regions is above 1,500 mm, while the annual rainfall in the eastern regions is below 1,000 mm. The variability of rainfall from east to west can also be seen in the image. For example, in 1990, the annual rainfall in the western regions was significantly higher than in the eastern regions. However, in 2020, the annual rainfall in the western regions was only slightly higher than in the eastern regions.

3.2. Correlation between rainfall variability and NDVI

The rainfall variability from year to year can significantly impact agriculture and water resources in Rwanda. For example, if there is a drought in the western regions, it can lead to crop failure and water shortages. The rainfall distribution in Rwanda is more variable in the eastern and western regions. This is because the eastern regions are more exposed to the prevailing winds, which can bring in moisture and dry air. Consequently, this rainfall variability is affecting crops and other plants; this means that the increase in rainfall leads to more farming activities carried on the ground so that people can live sustainably. These are shown in the following NDVI images: 2000, 2010, and 2020 (Figure 5).

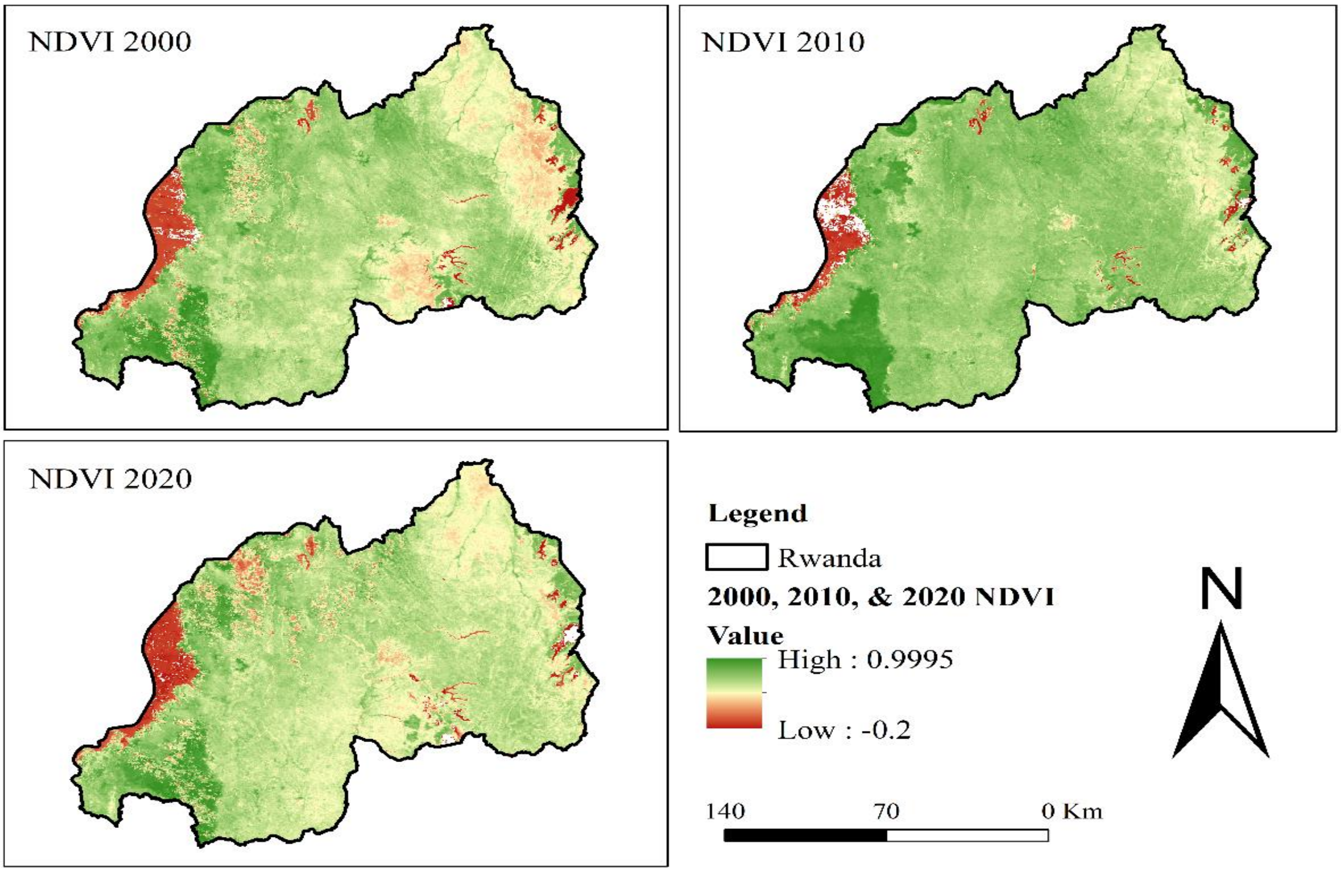

Figure 5: NDVI variation from 2000 to 2020

NDVI is a satellite-derived index that measures the amount of green vegetation on the Earth's surface. NDVI can be used to assess the health and productivity of crops. Climate change can cause changes in NDVI by affecting photosynthesis, evapotranspiration, and other plant physiological processes. High NDVI values indicate dense vegetation, while low NDVI values indicate sparse vegetation or no vegetation. The NDVI of Rwanda has decreased over the past 20 years. This is consistent with the fact that rainfall in Rwanda has also decreased during this period. The annual rainfall in Rwanda for 1990, 2000, 2010, and 2020 was 1160.1 mm, 1078.2 mm, 1402.4 mm, and 1391.1 mm, respectively. These values show that the annual rainfall in Rwanda can vary significantly from year to year. For example, the rainfall in 2010 and 2020 was significantly higher than in 1990 and 2000. NDVI image shows Rwanda had higher vegetation cover in 2010 and 2020 than in 2000. This is consistent with the recorded rainfall data, which shows that Rwanda had more rainfall in 2010 and 2020 than in 2000. Here is a more detailed comparison of the NDVI image and the rainfall data:

Table 3. Correlation of the NDVI image and the rainfall data

Years	Rainfall (mm)	NDVI level
2000	1078.2	Low
2010	1402.4	Very high
2020	1391.1	High

According to Table 3, there is a positive correlation between NDVI and rainfall. This is because NDVI measures vegetation health, which needs water to grow.

More water is available for vegetation when there is more rainfall, and NDVI is higher. The image shows that the highest NDVI values in Rwanda are found in the western and northwestern parts of the country. These areas also have the highest rainfall. This suggests that these areas are most suitable for agriculture. The eastern and southeastern parts of the country have lower NDVI values and rainfall. This suggests that these areas are less suitable for agriculture. However, some areas in these regions still have higher NDVI values, which suggests that agriculture is still possible but may require more irrigation or other management practices.

3.3. Rainfall variability in both seasons and months

Figure 6 and Figure 7 show the rainfall changes from 2000 to 2020 and rainfall variability and distribution from January to December.

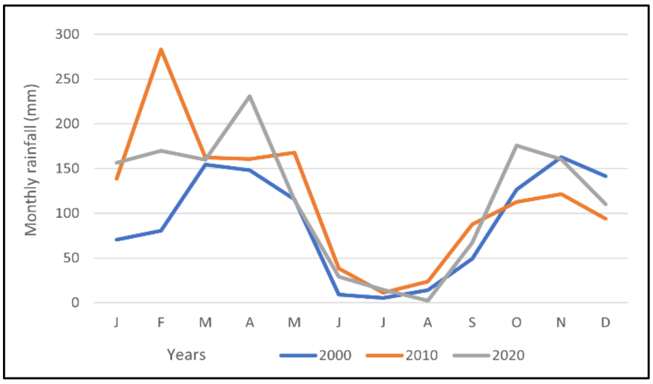

Figure 6: Monthly rainfall distribution and rainfall decreasing trend line (January to December)

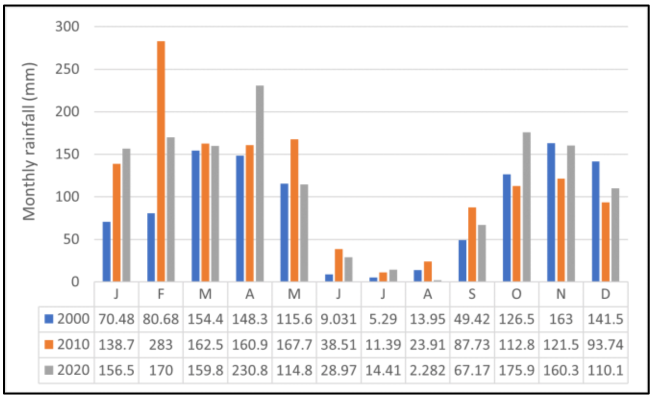

Figure 7: Monthly and Annual rainfall distribution and variation

According to Figures 6 & 7, MAM receives high rainfall, followed by SON, then DJF, and finally JJA. Generally, the country experiences two rainy seasons: a long rainy season from March to May (MAM) and a short rainy season from September to November (SON). During the long rainy season, the country experiences heavy rainfall, especially in the western and northwestern parts, while the eastern and southeastern parts receive less rainfall. The long rainy season is essential for agriculture, providing the necessary moisture for growing crops. The short rainy season is less intense than the long rainy season. During this time, the country experiences moderate rainfall. Also, Rwanda experiences two dry seasons each year, ranging from June to August (JJA) and December to February (DJF) (Muhire et al., 2018). During these times, the country receives very little rainfall. The dry seasons can be challenging for agriculture, as crops can suffer from drought. During the specified timeframe, Rwanda experiences abundant rainfall from September through the end of May, followed by a decline in precipitation from early June to late August. This pattern can negatively impact rain-fed agriculture due to irregular rainfall and droughts, resulting in water scarcity, crop loss, and diminished yields. Additionally, rural households dependent solely on subsistence farming are prone to experiencing reduced income levels, as they cannot generate surplus produce for the market (Ngango & Seungjee, 2021). During the dry season, growing upland crops can be tricky due to their specific water needs. At first, they require 30 millimeters of water each month, but as they grow, this jumps to 120 millimeters. Assuming the soil can hold 50 millimeters of water for every 75 centimeters of depth, we ideally need 100 to 140 millimeters of monthly rainfall to keep the crops healthy. This highlights the difficulty of providing the right amount of water during dry seasons (Oldeman & Suardi, 1977).

4. Conclusion and recommendations

As we observe the patterns in Rwanda, it becomes clear that there is a strong correlation between rainfall and vegetation cover. The gradual decrease in rainfall from the west to the east has a direct impact on the vegetation, with areas that receive higher rainfall boasting denser vegetation cover. This is particularly evident in the national parks and northwestern regions. Research has shown that there is a direct relationship between increased rainfall and augmented vegetation, while reduced rainfall leads to decreased vegetation cover. Moreover, it is evident that areas in the eastern province, which receive lower rainfall, suffer from diminished vegetation. Given the critical role of trees in influencing rainfall patterns, it is recommended that trees be strategically planted in regions with lower rainfall, particularly in the eastern areas. This intervention aims to mitigate the effects of drought and associated negative impacts by potentially influencing local rainfall patterns positively. In summary, this research underscores the pivotal relationship between rainfall and vegetation cover in Rwanda. It emphasizes the need to address areas with lower vegetation cover by implementing tree planting initiatives to combat drought and related adversities while leveraging the interconnection between trees and rainfall to foster a more balanced ecosystem across the country.

Funding

This study was funded and supported by the key program for international cooperation of the Bureau of International Cooperation, Chinese Academy of Sciences (Grant Number:151542KYSB20200018), the projects of the National Natural Science Foundation of China (NSFC Grant Number: U1703241), and the Sino-Africa Joint

Research Center of Chinese Academy of Sciences (Grant Number: SAJC202107).

Author contributions

Rosette Ambiance Shema: Conceptualization, Data curation, Writing-Original draft preparation, Methodology, and Software. **Li Lanhai:** Visualization, Investigation, Writing-Reviewing, Editing Validation.

Conflicts of interest

The authors declare no conflicts of interest.

Statement of Research and Publication Ethics

Research and publication ethics were complied with in the study.

References

Algur, K. D., Patel, S. K., & Chauhan, S. (2021). The impact of drought on the health and livelihoods of women and children in India: A systematic review. *Children and Youth Services Review,* 122, 105909. https://doi.org/10.1016/j.childyouth.2020.105909

Dehling, J. M., & Sinsch, U. (2023). Amphibians of Rwanda: Diversity, Community features, and conservation status. *Diversity*, 15(4), 512. https://doi.org/10.3390/d15040512

Gatwaza, O. C., & Wang, X. (2021). Mapping of biodiversity hubs and key ecosystem services as a tool for shaping optimal areas for conservation. *Plos One,* 16(8). https://doi.org/10.1371/journal.pone.0253151

Kalisa, W., Igbawua, T., Henchiri, M., Ali, S., Zhang, S., Bai, Y., & Zhang, J. (2019). Assessment of climate impact on vegetation dynamics over East Africa from 1982 to 2015. *Scientific Reports*, 9(1), 16865. https://doi.org/10.1038/s41598-019-53150-0

Kirchmeier-Young, M. C., & Zhang, X. (2020). Human influence has intensified extreme precipitation in North America. *PNAS*, 117(24), 13308–13313. https://doi.org/10.1073/pnas.1921628117

Kuradusenge, M., Kumaran, S., Zennaro, M., & Niyonzima, A. (2021). Experimental study of site-specific soil water content and rainfall inducing shallow landslides: Case of gakenke district, Rwanda. *Geofluids*, 2021, 1–18. https://doi.org/10.1155/2021/7194988

Maue, C. C. (2021). *Climate, agriculture, and economic development: Theories and methods for agricultural productivity analysis*. Stanford University.

Mountjoy, A. B., & Embleton, C. (2023). *Africa: A geographical study.* Taylor & Francis.

Muhire, I., Tesfamichael, S. G., Ahmed, F., & Minani, E. (2018). Spatio-temporal trend analysis of projected precipitation data over Rwanda. *Theoretical and Applied Climatology,* 131(1–2), 671–680. https://doi.org/10.1007/s00704-016-2002-8

de Dieu Ndayisenga, J., & Mupenzi, C. (2020). Analysis of rainfall and temperature at Kamembe in Western province of Rwanda. *East African Journal Science*, 10(10). https://doi.org/10.62103/eajst.v10i10.127

Ngango, J., & Seungjee, H. (2021). Adoption of small-scale irrigation technologies and its impact on land productivity: Evidence from Rwanda. *Journal of Integrative Agriculture*, 20(8), 2302–2312. https://doi.org/10.1016/S2095-3119(20)63417-7

NISR. (2023). *The fifth Rwanda population and housing census, main indicators report*. Retrieved December 03, 2023, from https://statistics.gov.rw/file/13787/download?token=gjjLyRXT

Oldeman, L. R., & Suardi, D. (1977). *Climatic determinants in relation to cropping patterns* [Symposium presentation]. IRRI Symposium on Cropping Systems Research and Development for the Asian Farmer.

Shahzad, L., Tahir, A., Sharif, F., Khan, W. U. D., Farooq, M. A., Abbas, A., & Saqib, Z. A. (2019). Vulnerability, well-being, and livelihood adaptation under changing environmental conditions: A case from mountainous region of Pakistan. *Environmental Science and Pollution Research*, 26, 26748–26764. https://doi.org/10.1007/s11356-019-05880-x

Shaw, J. A., Collins, S. L., Ohlert, T. J., Heavenrich, H., Cook, E., Wheeler, M. M., Grimm, N. B., & Hall, S. J. (2023). Seasonal rainfall, shrub cover and soil properties drive production of winter annuals in the Northern Sonoran Desert. *Ecosystems*, 1–17. https://doi.org/10.1007/s10021-023-00850-4

Siebert, A., Dinku, T., Vuguziga, F., Twahirwa, A., Kagabo, D. M., delCorral, J., & Robertson, A. W. (2019). Evaluation of ENACTS-Rwanda: A new multi-decade, high-resolution rainfall and temperature data set—Climatology. *International Journal of Climatology,* 39(6), 3104–3120. https://doi.org/10.1002/joc.6010

Yuan, L., Chen, X., Wang, X., Xiong, Z., & Song, C. (2019). Spatial associations between NDVI and environmental factors in the Heihe River Basin. *Journal of Geographical Sciences*, 29(9), 1548–1564. https://doi.org/10.1007/s11442-019-1676-0

Advanced GIS – 2024; 4(1); 31-41

Advanced GIS

http://publish.mersin.edu.tr/index.php/agis/index

e-ISSN:2822-7026

Assessment of flood susceptibility utilizing remote sensing and geographic information systems: A case study of Mpazi sub-catchment in the city of Kigali

Patience Manizabayo*[1], Hyacinthe Ngwijabagabo[1], Isaac Nzayisenga[2], Sabato Nzamwita[2], Laika Amani[1], Eugene Uwitonze[1], Katabarwa Murenzi Gilbert[3]

[1]*University of Rwanda, Environmental Planning, Spatial Planning, Kigali City, Rwanda*
[2]*University of Rwanda, Urban Planning, Spatial Planning, Kigali City, Rwanda*
[3]*Tongji University, Surveying, and Geo-informatics, Shanghai, China*

Keywords
GIS,
Flood Vulnerability,
Natural Disasters,
Spatial Overlay,
Climate Change

check for updates

Research / Review Article
Received: 03/12/2023
Revised: 21/02/2024
Accepted: 19/03/2024
Published: 02/04/2024

Abstract

The Mpazi sub-catchment has been facing recurring floods, which pose significant threats to the community and environment. However, GIS technology has proven to be a valuable tool in assessing flood risks and vulnerability in the region. By analyzing spatial data such as land use, elevation, and rainfall patterns, detailed flood maps can be generated to simulate flood scenarios and develop effective management plans. The study conducted in this region revealed that there is a high susceptibility to flood hazards, particularly during the rainy season. The study identified the most vulnerable areas in the region and categorized them as follows: very high risk (39.74%), high risk (13.02%), moderate risk (30.22%), low risk (5.12%), and very low risk (11.9%). It is important to note that floods not only impact the environment but also infrastructure, such as residential and commercial buildings. The insights provided by this study are invaluable for stakeholders in developing effective flood management strategies to mitigate. Hence, all concerned government departments and citizens should collaborate actively to alleviate the ongoing rise in flooding and its impact. Adherence to land use and zoning regulations is crucial in this regard to address the issue effectively.

1. Introduction

Globally, many people are exposed to high vulnerability to natural disasters and other environmental changes because of climate change (Wali et al., 2013). This is because the climate has changed and is continuously changing on a global basis, and as a result, there are natural increases in the frequency and severity of natural disasters (Estrada et al., 2023). They are the most common natural disasters that occur when the river channel receives much more water than the usual amount it can receive (Andrews et al., 2017). The result of excessive rainfall is that the rivers rise, and a flood develops because the river cannot handle the extra water, causing flooding everywhere along the river's path. The result of excessive rainfall is that the rivers rise, and a flood develops because the river cannot handle the extra water, causing flooding everywhere along the river's path (Wali et al., 2013). This implies that all elements at risk such as population are highly affected by floods i.e., the more vulnerable a population is, the more likely they are to suffer the consequences of a flood event (Cutter et al., 2008). The areas with high levels of poverty and inadequate infrastructure are more vulnerable to floods and experience higher impacts. For example, low-income areas in urban environments are often at high risk of flooding and have higher levels of vulnerability due to factors such as poor drainage systems and lack of access to information (Bubeck et al., 2012).

Similarly, the vulnerability of critical infrastructure such as hospitals and schools is a key factor in determining the impact of floods on communities, and therefore, the more critical infrastructure that is damaged or destroyed, the more difficult it is to provide emergency services and restore regularity (Pant et al., 2018). Moreover, vulnerability and exposure to flood risk are important factors in determining the impact of floods

***Corresponding Author**

*(manizabayopatience08@gmail.com) ORCID 0009-0000-5283-5358
(ngwijabagabohyacinthe@gmail.com) ORCID 0000-0003-1530-9302
(nzayisaac85@gmail.com) ORCID 0009-0009-2284-9834
(nzamwitasabbath@gmail.com) ORCID 0009-0004-7138-0386
(amanilaika01@gmail.com) ORCID Not available
(eugeneuwitonze02@gmail.com) ORCID 0000-0002-4630-3379
(hata2020@tongji.edu.cn) ORCID 0009-0005-4789-275X

Cite this article

Manizabayo, P., Ngwijabagabo, H., Nzayisenga, I., Nzamwita, S., Amani, L., Uwitonze, E., & Gilbert, K. M. (2024). Assessment of flood susceptibility utilizing remote sensing and geographic information systems: A Case Study of Mpazi Sub-catchment in the City of Kigali. *Advanced GIS,* 4(1), 31-41.

on agricultural production; this is to say that areas with higher vulnerability and exposure to flood risk experience more significant reductions in agricultural productivity following a flood event (Wang et al., 2013).

Many African countries are particularly vulnerable to flooding, which is made worse for several reasons, including climate change, urbanization, deforestation, and inadequate infrastructure (Pörtner et al., 2019). Africa is the continent most affected by floods, with an average of 3.4 million people affected annually between 2000 and 2018, the number of flood events in Africa has also been increasing, with a 50% increase in the frequency of floods between 1995 and 2015 (Loke et al., 2021). Floods in Africa often result in significant economic and social impacts, with loss of life, damage to infrastructure and property, and disruption of livelihoods. In many cases, vulnerable communities are disproportionately affected, with women and children being particularly at risk (Pörtner et al., 2019). By the end of the 20th century, the research examined the impact of climate change on flood hazards in West Africa and found that flood frequency and magnitude are projected to increase significantly, with the potential to affect millions of people, and the study also emphasized the need for proactive flood risk management strategies to mitigate the potential impacts of climate change on vulnerable communities in the region (Alfieri et al., 2016).

In East Africa, flood vulnerability is a significant issue affecting millions of people every year. The region is prone to floods due to heavy rainfall, poor drainage systems, deforestation, and climate change. Flood events in East Africa have had devastating impacts, including the destruction of homes and infrastructure, contamination of water sources, and an increased risk of illness (Birmah et al., 2021). In 2015, heavy rains caused severe flooding in several East African countries, including Ethiopia, Kenya, and Somalia; as a result, over 100,000 people were affected, and at least 40 people died because of the floods (Gamoyo et al., 2015); and in 2017, over 300,000 people were displaced, and at least 100 people died because of the floods (UNICEF, 2018). While flood hazard is natural, human influence in the variation and modification of urban space worsens the problem where the terrible consequences are dependent on the degree of human activities and occupancy in vulnerable areas (Cirella et al., 2018; Mashi et al., 2020; Wahab & Falola, 2022).

Nyabugogo watershed, particularly Mpazi sub-catchment the focus of this research has experienced flooding in several incidents. This is mostly because Mpazi sub-catchment is located at a low altitude relative to its surroundings and the peculiarities of the Kigali city drainage system convergence zone, which has frequently experienced flooding (Gerard, 2014). When flooding happens in this region, the damaged materials and the soil eroded from the upper stream flow with the water through the river channel, and as a result, they are deposited downstream, ultimately closing the drainage channels (Manyifika, 2015). All the materials and eroded soil cause the channel to be blocked, and the water cannot flow as it should, which causes the surrounding area to flood. Mpazi channel, which receives upstream rainwater, is one of the main causes of flooding in this area. Since the channel is blocked by debris, eroded soil, and damaged materials, the water cannot, therefore, flow as it should, which suddenly causes the surrounding areas to flood. The Nyabugogo River, especially the Mpazi channel, which receives rainwater from upstream, is one of the main causes of flooding in this area (Gerard, 2014). All the rainwater from Gitega, Kimisagara, Muhima, and Nyabugogo areas falls into Nyabugogo River during the rainy season, and this leads to frequent floods in this area, which are known as flash floods. Flash floods are sudden, rapid floods that can occur within a few minutes or hours of heavy rainfall or other causes of rapid water accumulation; these floods are highly dangerous and destructive, as they often catch people off guard and can quickly overwhelm infrastructure and buildings. Flash floods typically occur in low-lying areas or in as with poor drainage, and they can be triggered by intense rainfall, dam, or levee failures, or other natural or man-made factors that cause a sudden influx of water (Alarifi et al., 2022; Mind'je et al., 2019). About 8 km^2 of the urban area is drained to the Nyabugogo River. Eventually, it is characterized by flash floods, which suddenly put people at risk and destroy socio-economic infrastructures (Manyifika, 2015; Habonimana et al., 2015).

Geographical Information system (GIS) is a critical tool in flood management (Peker et al., 2024). Floods are major natural disasters that can cause significant damage to communities, infrastructure, and the environment (Njogu, 2021). The increasing frequency and severity of floods, attributed to climate change, have led to a growing need for effective flood management strategies (Dub et al., 2022). Geographical Information System has emerged as a powerful tool to support flood management, providing valuable information and analysis to decision-makers to support the planning and response to floods (Bilașco et al., 2022). GIS is used for various purposes in flood management, starting with flood risk assessment, where GIS analyzes topographical, hydrological, and meteorological data to identify high-risk areas and develop risk reduction strategies (Hadipour et al., 2020).

Subsequently, GIS is used to create flood hazard maps, which are generated by analyzing elevation, slope, land use, soil type, and rainfall data, among others, providing useful information for planning and responding to floods (Poussin et al., 2015). Real-time flood monitoring is another application of GIS in flood management. It involves using remote sensing, and citizen-generated data to identify areas that require immediate attention and to inform emergency response efforts (Khedo, 2013). Furthermore, GIS is used to develop early warning systems that provide timely and accurate information about potential floods, issuing alerts to communities and decision-makers, and is used to develop flood risk reduction strategies such as the construction of flood protection infrastructure, land use planning, and public education campaigns, aiming to minimize the impact of floods on communities and reduce the risk of flooding (Cai et al., 2021).

This study intends to combine geospatial data to identify flood vulnerability areas located in flood-prone areas. In past research that attempted to examine flood vulnerability in Mpazi sub-catchment, the use of GIS technology to display flood-prone areas was insufficient. This knowledge gap motivates this study to use GIS-based analysis to map flood-prone areas within the Mpazi sub-catchment sufficiently. The insufficient use of GIS-based vulnerability assessments in flood-prone areas of the Mpazi sub-catchment presents a knowledge gap that this study aims to address. This study intends to combine geospatial data to identify flood vulnerability areas located in flood-prone areas by using the GIS-AHP method, to provide valuable information to contribute to the development of effective flood risk management strategies in the region and eventually help policymakers to take some coping strategies and adaptive measures to reduce flood risks. This literature synthesis presents key findings, and contributions from different studies, highlighting the complex interplay between vulnerability, climate dynamics, and the role of GIS tools in effective flood risk assessment and management (Table 1).

Table 1. Research literature summary

Reference	Key findings	Contribution to research
(Wali et al., 2013)	Climate change contributes to increased vulnerability to natural disasters globally	Linking between climate change and heightened vulnerability to natural disasters.
(Estrada et al., 2023)	Ongoing global climate change leads to a rise in the frequency and severity of natural disasters.	Emphasizes the continuous impact of climate change on the frequency and severity of natural disasters.
(Peker et al., 2024)	GIS is a critical tool in flood management, offering support in flood risk assessment, hazard mapping, real-time monitoring, and early warning systems.	Recognizes GIS as a powerful tool in various aspects of flood management, including assessment and monitoring.
(Manyifika, 2015)	Flooding in Mpazi sub-catchment leads to debris and eroded soil blockages in the river channel, causing flash floods and extensive damage in downstream areas.	Describes the consequences of flooding in Mpazi sub-catchment, specifically the occurrence of flash floods due to channel blockages.

2. Materials and method

2.1. Study area

The study is concentrated on the Mpazi sub-catchment, which is wholly enclosed inside the Nyarugenge district (Figure 1, 2). One of the Nyabugogo catchment sub-catchments, the Mpazi sub-catchment, lies between 10 56'15" and 10 58'45"S and between 300 02'00'E and 300 03'45"E. This sub-sub-catchment is found in Nyarugenge District in western Kigali City and covers an area of 888.90 ha.

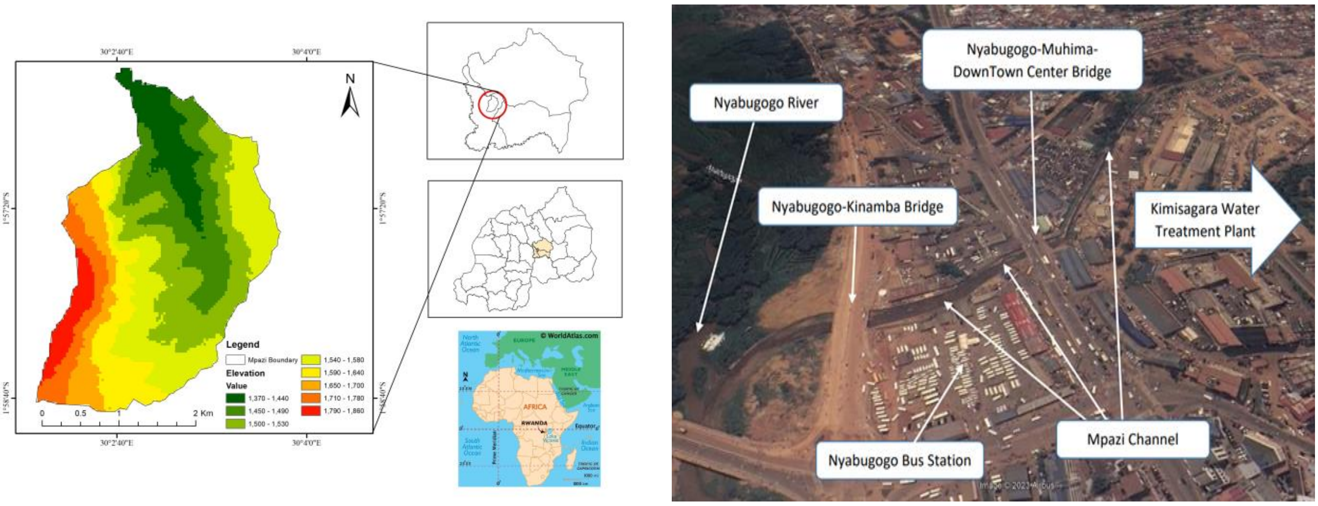

(a) (b)

Figure 1. (a) Study area, (b) Mpazi sub-catchment downstream (Google Earth Pro, 2023)

In Mpazi sub-catchment, the average annual temperature ranges from 16°C to 20°C, its climate is defined by two rainy seasons that typically last from February to May and from mid-September to mid-December with approximately 1,250 to 1,300 mm of rain falling on average each year (Balana et al., 2020). As compared to the rest of the watershed, the Mpazi section is estimated to have the highest peak runoff discharge (flow) at 107.5 m^3/s for 25 years (Habonimana et al., 2015). The geological structure is composed of meta-sedimentary and granite rocks such as schist, sandstones, and siltstones (Balana et al., 2020). Hillside surfaces are covered in lateritic soils that are rich in iron and aluminum, while lowlands and wetlands have alluvial and organic soils (Bizimana, & Ndahigwa, 2020).

2.2. Data processing methods

Choosing the right factors or criteria is crucial for a detailed flood vulnerability assessment. This is particularly important in identifying and mapping natural hazards such as landslides, floods, and cyclones, which rely on various factors for their occurrence. To create an accurate flood vulnerability map for a particular catchment area, it is imperative to carefully select the most appropriate factors (Rimba et al., 2017; Roy & Blaschke, 2015; Shivaprasad et al., 2018).

However, this can be challenging, as selecting parameters that consistently produce accurate susceptibility maps requires careful consideration and attention to detail. The selection of criteria and alternatives for flood vulnerability assessment in the Mpazi sub-catchment was based on a detailed literature review, data availability, and their relevance and impact on flood vulnerability. The analysis of vulnerability in this study focuses on the physical and natural factors that control and influence it. These factors have been identified and selected as criteria for the analysis. The study has identified five vulnerability criteria from different sources. The land use and cover map of the study area was delivered from data produced by Rwanda GeoPortal 2020. Slope data and elevation map were generated from Digital Elevation Model (DEM) data obtained from the United States Geological Survey portal (USGS). The precipitation map of the study area was delivered from the interpolation of data from Meteo Rwanda. To process and prepare the numerous spatial criterion layers, ArcGIS software (version 10.8) was used. The Analytical Hierarchy Process (AHP) technique is a GIS-based decision-making method and was delivered to weigh the criteria based on the information gathered during the field survey and literature review. This enabled the development of a more accurate and comprehensive assessment of flood vulnerability in the Mpazi sub-catchment.

TIFF Web-based Data derived from the Esri Land Cover-Living Atlas for Land Use and Land Cover (LuLc) is presented at a spatial resolution of 10 meters. This means that each pixel in the imagery represents an area on the Earth's surface with dimensions of 10 meters by 10 meters. STRM-DEM (Shuttle Radar Topography Mission - Digital Elevation Model) obtained from the USGS Earth Explorer has a spatial resolution of 10 meters. This indicates that each pixel in the digital elevation model corresponds to a 10-meter-by-10-meter area on the ground (Table 2).

Table 2. Data types and sources

Data Type & Resolution	Source	Period	Mapping Output
TIFF Web-based Data (10m Resolution)	Esri Land Cover-Living Atlas	2019-2021	LuLc
STRM-DEM (10m Resolution)	USGS Earth Explorer	2023	Elevation and Slope
Precipitation	Meteo Rwanda	2021	Precipitation
River buffers	Google Earth Pro	2023	Proximity analysis

2.3. Identification of criteria

Land use, particularly the built-up areas, is a critical factor that influences flooding in the study area. When natural surfaces such as vegetation and soils are replaced by impervious surfaces such as concrete and asphalt, the surface runoff increases, leading to more flooding. In the Mpazi sub-catchment, built-up areas also reduce the amount of infiltration, causing more water to flow into the streams and rivers, increasing the volume of water, which causes flooding, especially in low-lying sub-catchment areas. Generally, low-lying areas with gentle slopes are more susceptible to flooding than those with higher elevations and steeper slopes (Hu et al., 2017) (Figure 2).

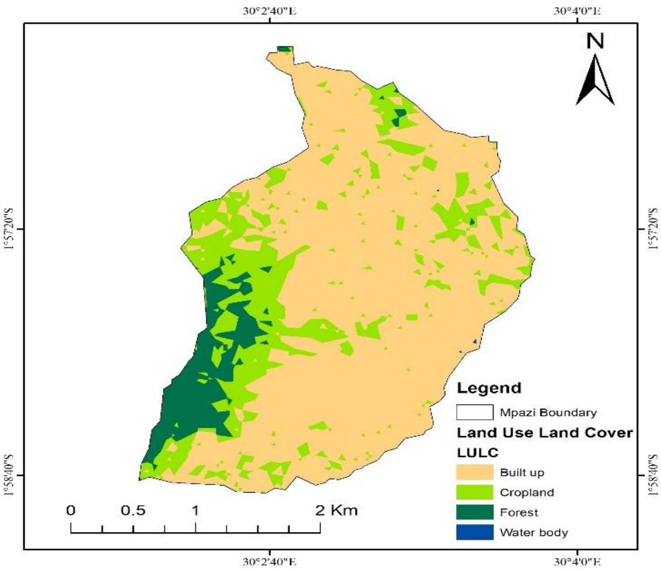

Figure 2. LuLc map

Another important flood risk factor is distance from the river channel (Figure 3). The lower the distance from the river, the higher the flood risk level. Precipitation is crucial to flood risk. When the precipitation increases, the flood risk also is higher (Rimba et al., 2017).

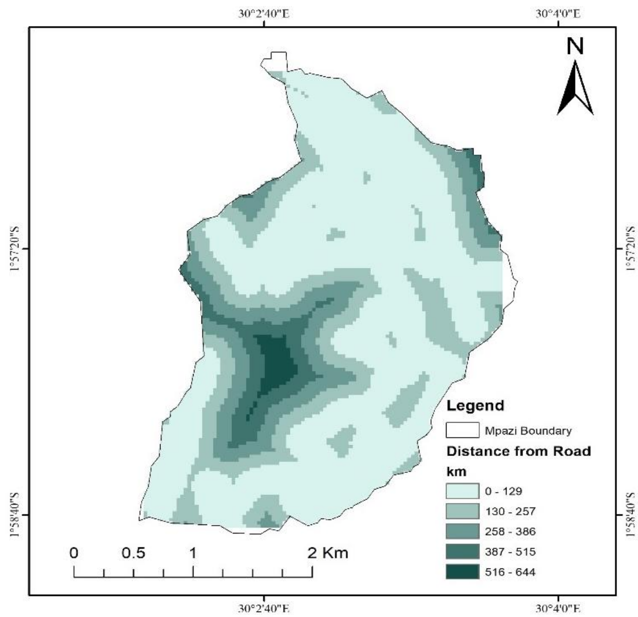

Figure 3. Flood criteria map distance from river

The Topographical Wetnex Index is another important factor that contributes to flood vulnerability. The topographic wetness index (TWI) is crucial in flood vulnerability assessment. TWI measures the land's capability to retain water and indicates areas of potential water accumulation during flooding events. Considering the TWI in flood vulnerability assessments, it is possible to identify low-lying areas with poor drainage and higher flood susceptibility. Areas with high TWI values are likely to have higher water saturation, resulting in increased vulnerability to flooding. Additionally, TWI can help prioritize flood mitigation efforts and inform land use planning by identifying areas where development should be avoided or proper water management measures should be implemented. The study area with levels >2-7 tends to be wet and more vulnerable to risk compared to areas with low wetness (Figure 4).

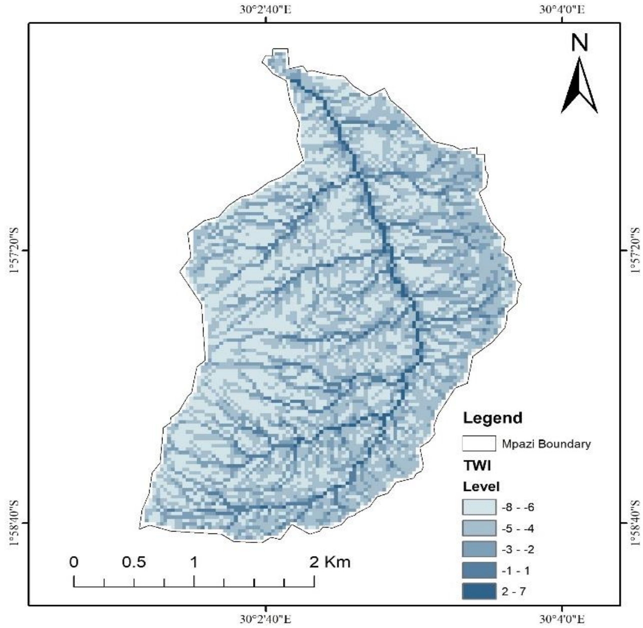

Figure 4. Topographical Wetnex Index map

The influence of slope and elevation in flood vulnerability assessment is significant. Slope affects the speed and direction of water flow during floods, impacting the intensity and spread of flooding. Areas with steeper slopes tend to channel water more rapidly, increasing flood hazards. Elevation is crucial in flood vulnerability, as low-lying areas are more prone to inundation (Figure 5).

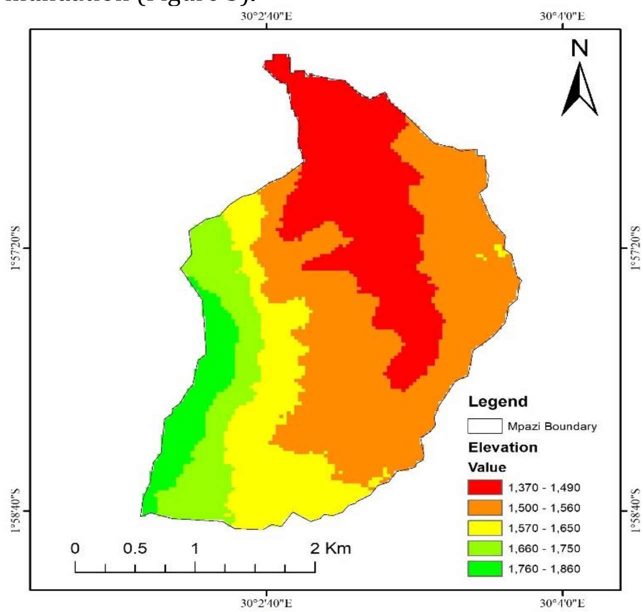

Figure 5. Elevation map

Higher elevations offer natural protection from flooding. Generally, low-lying areas with gentle slopes are more susceptible to flooding than those with higher elevations and steeper slopes (Hu et al., 2017) (Figure 6).

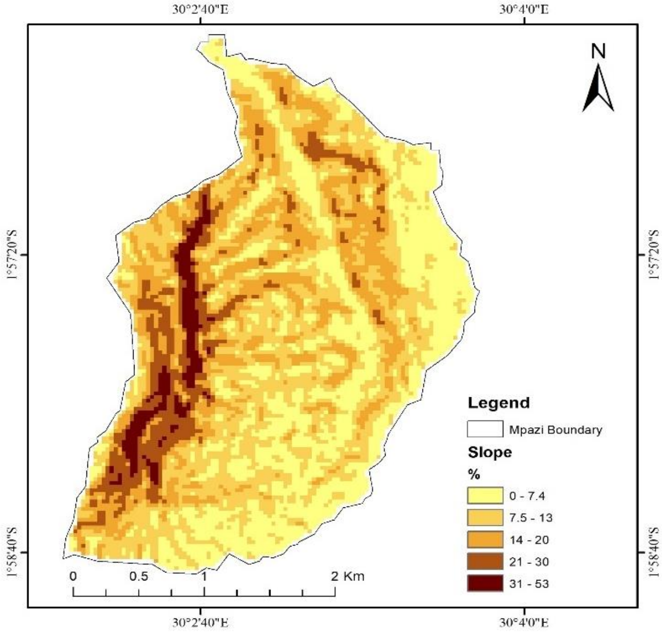

Figure 6. Slope map

Precipitation intensity is a crucial criterion that has a significant impact on the level of flood vulnerability (Rimba et al., 2017). Regions that experience higher levels of precipitation intensity are at a greater risk of flooding compared to areas with lower levels of precipitation intensity (Figure 7).

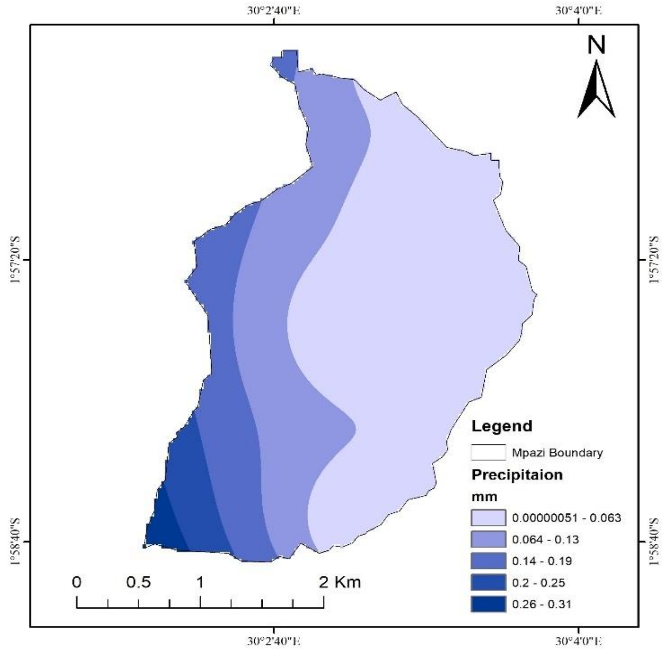

Figure 7. Precipitation map

Table 3. Scale of relative importance (adapted from Saaty (Saaty, 2002))

Relative Importance	Definition	Description
1	Equal importance	Two factors equally influence the objective
3	Moderate importance	Experience and judgment slightly favour one factor over another
5	Strong importance	Experience and judgment strongly favour one factor over another
7	Very strong importance	One decision factor is strongly favoured over another, and its supremacy is established in practice
9	Extreme importance	The evidence favouring one decision factor over another is of the highest possible orders of validity
2, 4, 6 and 8	Intermediate values between adjacent judgement	When compromise is required

The study has recognized the significance of these factors and aims to integrate them into the assessment of flood vulnerability by creating spatial thematic layers. The results of our GIS analysis reveal that areas with low elevations and steep slopes are highly vulnerable to flooding, which is consistent with previous studies. In this research, the Analytic Hierarchy Process (AHP) methodology was used to assign weights to the criteria for flood vulnerability (Table 3-5). The construction of pairwise comparison matrices was undertaken to quantify the criteria weights, drawing upon qualitative assessments provided by five experts and a user. The criteria were assigned weights based on the scale of relative importance proposed by Saaty (Saaty, 2002).

Table 4. Comparison matrix for flood risk criteria

Criteria	LuLc	Precipitation	Slope	TWI	Elevation	Distance from River
LULC	1	3	3	3	3	3
Precipitation	1/3	1	1/3	1/3	1/3	1/3
Slope	1/3	3	1	1/3	1/3	1/3
TWI	1/3	3	3	1	1/3	1
Elevation	1/3	3	3	3	1	3
Distance from River	1/5	1/3	1/3	1/3	1/3	1/3

Table 5. Flood risk classes and weights

Criteria	Unit	Very High	High	Moderate	Low	Very Low	Weights
LuLc	Level	Waterbody	Agricultural land	Built-Up	Bare land	Vegetation	0.178
Precipitation	mm	0.26 – 0.31	0.2 – 0.25	0.14 – 0.19	0.1-0.13	<0.1	0.262
Slope	%	0 – 7.2	7.3 – 13	14 – 20	21 – 30	31 - 53	0.145
TWI	Level	2 - 7	-1 – 1	-3 - -2	-5 - -4	-8 - -6	0.090
Elevation	m	>1370 – 1490	1500 – 1560	1570-1650	1660 - 1750	1760 - 1860	0.100
Distance from river	m	<129	>130 – 257	>258 – 386	>387 – 515	>516 - 644	0.225

3. Results

Choosing the right factors or criteria is crucial in conducting a detailed flood vulnerability assessment. This is particularly important in identifying and mapping natural hazards such as landslides, floods, and cyclones, which rely on various factors for their occurrence (Roy & Blaschke, 2015). By comparing the criteria weighted with the highest influence on flooding risk in the study area were calculated, precipitation (0.262); distance from the river (0.225); LuLc (0.17); slope (0.145); elevation (0.1); TWI (0.09). The flood vulnerability map identifies the most vulnerable areas to flooding in the study area, very high risk 39.74% (353.34 ha), high risk 13.02% (115.73 ha), moderate risk 30.22% (268.62 ha), low risk 5.12% (45.51 ha), very low risk 11.9% (105.77 ha) (Table 6).

Table 6. Flood risk areas in Mpazi sub-catchment

Flood Risk Classes	Area (km^2)	Rate (%)
Very Low	105.77	11.90
Low	45.51	5.12
Moderate	268.62	30.22
High	115.73	13.02
Very High	353.34	39.74

According to the field survey, infrastructures such as residential houses, trading centers, roads and bridges are frequently affected by flooding (Figure 8).

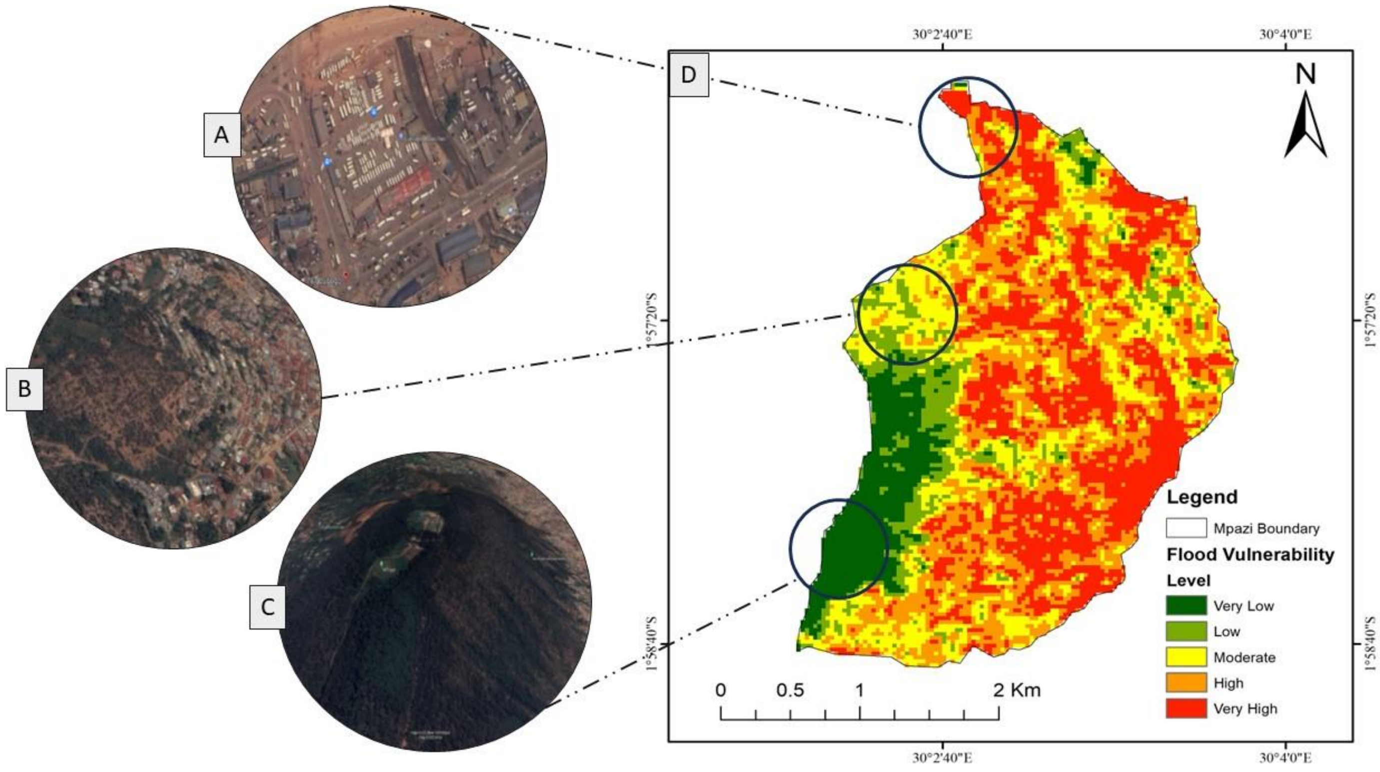

Figure 8. Flood risk map of Mpazi sub-catchment

The flood vulnerability map produced in this study for the Mpazi sub-catchment indicates that the area is highly susceptible to flooding. The map reveals that the highest flood vulnerability is concentrated in the eastern and northeastern parts of the sub-catchment, which are predominantly urban areas. These areas have high population densities, the land is mostly covered by impervious surfaces such as buildings, roads, and pavements. The flood vulnerability map produced in this study for the Mpazi sub-catchment indicates that the area is highly susceptible to flooding. The map reveals that the highest flood vulnerability is concentrated in the eastern and northeastern parts of the sub-catchment, which are predominantly urban areas. These areas have high population densities, and the land is mostly covered by impervious surfaces such as buildings, roads, and pavements. The study also found that the areas with the highest flood vulnerability are near the Nyabugogo River, which is prone to flooding during heavy rainfall. Additionally, the map shows that areas with steep slopes and poor soil drainage are also highly vulnerable to flooding. On the other hand, the western and southwestern parts of the sub-catchment have a lower flood vulnerability, as they are characterized by low population densities, agricultural land use, and gentle slopes. The results of this study highlight the need for effective flood management strategies in the highly vulnerable areas of the sub-catchment, particularly in urban areas with high population densities.

The areas which are more vulnerable to flooding are affected by the floods and loss of lives. Floods result in loss of life due to drowning or other flood-related injuries. People in highly vulnerable areas may be more likely to be caught off-guard by flooding, increasing the risk of fatalities (Habonimana et al., 2015). Damage to infrastructure; roads, bridges, and other infrastructure in highly vulnerable areas (Figure 8) making it difficult for emergency responders to access affected areas. This can also disrupt supply chains and commerce, leading to economic losses. In addition, in more vulnerable to flooding areas, floods lead to loss of property where they destroy or damage homes, businesses, and other property, leaving people without shelter or possessions. This can be especially devastating for those in highly vulnerable areas who may not have insurance or other resources to recover from such losses. Loss of property, floods can destroy or damage homes, businesses, and other property, leaving people without shelter or possessions. This can be especially devastating for those in highly vulnerable areas who may not have insurance or other resources to recover from such losses. Therefore, the effects of floods in highly vulnerable areas of Mpazi sub-catchment can be devastating and long-lasting. It is important to take steps to mitigate the risks of flooding, including improved infrastructure, early warning systems, and disaster preparedness planning.

4. Discussion

The areas which are more vulnerable to flooding are those very close to the active river channel. Also, the lowlands (low elevated areas) areas are at high risk because of overflow of water (Figure 8a). The reverse is true, which means the areas with high elevation are likely to have vegetation cover and this place is not more vulnerable to flooding (Figure 8c). The frequency, intensity, and impact of flooding are growing and causing more negative impacts on humans, the economy, and the environment (Mind'je et al., 2019).

A combination of engineering measures and nature-based solutions is essential to reduce flood risk effectively. Constructing retaining walls and planting vegetation cover are vital components of flood risk reduction, as they help to manage water flow and prevent erosion. However, in addition to these conventional approaches, developing nature-based solutions like Natural Water Retention Measures (NWRM) and Natural Flood Management (NFM) is becoming increasingly crucial. NWRM enhances natural features like wetlands and forests to absorb excess water. Natural water retention measures are "a multifunctional form of green infrastructure that can play an important role in catchment-scale flood risk management natural means and processes" (Taramelli et al., 2019). They include afforestation of upstream catchments; targeted planting for catching precipitation; maintenance of riparian buffers; urban forests; Land-use conversion for water quality improvements; green roofs and walls; rainwater harvesting; permeable paving; swales; soak ways; infiltration trenches; rain gardens; growth of urban green spaces; detention basins; permeable paving; retention ponds; urban channel restoration; etc. (Seddon et al., 2020).

NWRM can be performed for flood risk reduction either within Mpazi sub-catchment, for instance, the green roof is designed to intercept rainfall since it is slowed as it passes through the vegetation (Zeleňáková et al., 2017) and it can be implemented into very high-risk areas especially the low-lying slope of the region. The drainage layer stores some of the rainwater, which is then absorbed by the vegetation and the remaining water is then released from the roof as usual. In comparison to a normal roof, the flow rates from a green roof are lower and attenuated, and the total volumes discharged from the roof are lower (Figure 9a). Therefore, green roofs catch rainwater at their source and serve as the foundation of sustainable flood control management; permeable paving is made to allow rainwater to permeate through the surface into the soils beneath it to facilitate more infiltration. It can most be frequently employed on road networks and parking areas (Mohammadreza Hassani et al., 2017). Permeable paving can be practiced in Nyabugogo car park. The main purpose of channels is to capture runoff, permit sediment deposition, and transport the runoff to features farther downstream in the sustainable drainage network (Collentine & Futter, 2018) and it can be helpful when implemented around Nyabugogo car park where during heavy rainfall, runoff water is captured through drainage channels to reduce water from floating Stone-filled infiltration trenches (Figure 9d) are made up with sands and gravels, can assist recharge groundwater, maintain river base flow, and minimize runoff volumes and rates (Mashi et al., 2020), and those infiltration trenches are typically well suited for areas that generate large amounts of sediment especially low-lying areas near Nyabugogo commercial market; and this can be employed (Figure 9b).

Figure 9. (a) Green roof; (b) Permeable paving; (c) Channels; (d) Stone-filled infiltration trenches

Natural Water Resources Measures (NWRM) in general boost soil infiltration, delay overland flow, lower channel velocity, and raise evapotranspiration to change the hydrological cycle's rate and restore the landscape's ability to retain water. Both the frequency and the intensity of floods may be reduced because of these processes (Ribas et al., 2020). NFM focuses on working with the landscape to slow down and naturally store floodwaters. As an illustration of a nature-based solution, this study intends that Natural Flood Management (NFM) be promoted as a risk reduction method to help widespread sustainable flood risk management within Mpazi sub-catchment. NFM is one type of nature-based solution (NBS) that serves as an "umbrella concept" for a variety of ecosystem-related strategies for resolving societal issues (Wilkinson et al., 2019). This nature-based solution is one of many strategies being looked at internationally to lower flood risk. NFM encompasses a wide range of actions that change, repair, or make use of landscape elements to control flood risk. NFM seeks to manage floodwater sources and channels by collaborating with catchment-wide hydrological and morphological processes (Holstead et al., 2017). Moreover, it encompasses actions that "alter, restore, or use landscape features to manage flood (Figure 9c). Natural flood management strives to utilize and collaborate with natural processes to lower flood risk while also bringing about broader improvements in the environment and social and economic advantages in river catchments (Collentine & Futter, 2018) by using GIS to highlight the areas of attention and priority in Mpazi basin to implement this kind of nature-based solutions to reduce flood risks.

As a result, NFM may use a wide range of approaches, such as restoring upland mires, altering land use, planting trees, managing sediment, storing runoff, restoring rivers, and utilizing washlands (Holstead et al., 2017). Natural Flood Management (NFM) emerges as a sustainable and innovative approach to mitigate the risk of flooding in the highly flood-prone areas of the Mpazi sub-catchment. At its core, NFM involves the strategic deployment of ecosystem-based solutions that harmonize with the natural landscape. Afforestation along the river channel, a key component of NFM, entails the deliberate planting of trees and vegetation upstream. The roots of these plants act as natural barriers, absorbing excess rainfall and reducing surface runoff. This not only helps in stabilizing the soil but also aids in regulating the flow of water, preventing it from rapidly descending downstream of Mpazi channel. This overarches goal of NFM in the Mpazi sub-catchment is to restore and enhance watershed processes that have been adversely affected by human interventions. These interventions, such as deforestation and urbanization, have disrupted the natural balance of the ecosystem. By re-establishing these processes, NFM not only lessens the immediate flood risk but also promotes long-term resilience and sustainability in the face of climate change. As communities grapple with the escalating challenges of unpredictable weather patterns, embracing NFM offers a holistic and nature-based solution to foster a harmonious coexistence between human settlements and the surrounding environment (de Boer et al., 2015). By integrating these nature-based approaches with developed infrastructure, a more resilient and sustainable flood management system is created, safeguarding communities and the environment from the growing threat of floods.

5. Conclusion

Flooding can have a wide-ranging and severe impact on various sectors and communities. Human settlements and shelters are vulnerable to damage or displacement, threatening people's safety, and well-being. Health and nutrition, water and sanitation, education, agriculture, and infrastructure can all be disrupted or damaged, affecting the basic needs and services of the affected population. Small and medium-sized enterprises suffer losses and can struggle to recover. Moreover, flooding threatens human life, carries health risks from contaminants, and causes long-term environmental effects through erosion and habitat disruption. The economic impact can be substantial, affecting both the government and private sector. To address these issues, utilizing GIS for flood vulnerability assessment is essential. This approach helps identify high-risk areas and informs strategies for reducing the impacts through better preparedness, improved infrastructure, and sustainable land use planning. The flood vulnerability assessment in Mpazi sub-catchment reveals an urgent high-risk situation, with 80% vulnerability.

Priority recommended measures include nature-based solutions like wetland restoration, integrated GIS-based flood management, public awareness campaigns, and infrastructure development. Land use planning, coupled with continuous monitoring, provides a systematic framework for sustainable development. It enables the identification of high-risk zones, guiding informed decisions on urban expansion and infrastructure placement. Collaboration among stakeholders, including government bodies, non-governmental organizations (NGOs), and local communities, is fundamental to the success of these measures. Encouraging future research on Participatory GIS is recommended, it does not only advance scientific understanding but also strengthens community engagement, ensuring that local knowledge and perspectives are integral to the development and implementation of flood mitigation strategies. These measures collectively mitigate flooding risks, fostering sustainable development, and ensuring resident safety in flood-prone areas.

Acknowledgement

The authors extend their heartfelt appreciation to the referenced authors and Meteo Rwanda for their valuable contributions to the research. Furthermore, the authors wish to recognize the editor and anonymous reviewers for their insightful feedback, which greatly enhanced the overall quality of the final manuscript.

Author Contributions

Patience Manizabayo, Laika Amani and Eugene Uwitonze: Literature review, field study, methodology, software, and data processing. **Isaac Nzayisenga and Sabato Nzamwita:** Revision, data validation, visualization and interpretation. **Nzayisenga Isaac, Hyacinthe Ngwijabagabo and Katabarwa Murenzi Gilbert:** Reviewing, editing, and final draft.

Statement of Conflicts of Interest

There is no conflict of interest between the authors.

Statement of Research and Publication Ethics

Research and publication ethics were complied with in the study.

References

Alarifi, S. S., Abdelkareem, M., Abdalla, F., & Alotaibi, M. (2022). Flash flood hazard mapping using remote sensing and GIS techniques in Southwestern Saudi Arabia. *Sustainability*, *14*(21). https://doi.org/10.3390/su142114145

Alfieri, L., Bisselink, B., Dottori, F., Naumann, G., De Roo, A., Salamon, P., Wyser, K., Feyen, L., & Alfieri, L. (2016). *Global projections of river flood risk in a warmer world*. https://doi.org/10.1111/eft2.183

Andrews, J., Babb, D., & Barber, D. G. (2017). Climate change and sea ice: Shipping accessibility on the marine transportation corridor through Hudson Bay and Hudson Strait (1980-2014). *Elementa: Science of the Anthropocene*, 5(15). https://doi.org/10.1525/elementa.130

Balana, B. B., Bizimana, J. C., Richardson, J. W., Lefore, N., Adimassu, Z., & Herbst, B. K. (2020). Economic and food security effects of small-scale irrigation technologies in northern Ghana. *Water Resources and Economics*, 29, 100141. https://doi.org/10.1016/j.wre.2019.03.001

Bilașco, S., Hognogi, G.-G., Roșca, S., Pop, A.-M., Iuliu, V., Fodorean, I., Marian-Potra, A.-C., & Sestras, P.

(2022). Flash flood risk assessment and mitigation in digital-era governance Using unmanned aerial vehicle and GIS spatial analyses case study: Small river basins. *Remote Sensing,* 14(10), 2481. https://doi.org/10.3390/rs14102481

Birmah, M. N., Kigun, P. A., Alfred, Y. B., St, M., & Surajo, L. A. (2021). Flood assessment in Suleja local government area, Niger state, Nigeria. *International Journal of Research Publication and Reviews,* 2(3), 219-239.

Bizimana, J. P., & Ndahigwa, E. (2020). Cadastral information and erosion modeling for monitoring Gullies in Mpazi catchment area, Kigali city. *Rwanda Journal of Engineering, Science, Technology and Environment*, *3*(1), 81-106. https://doi.org/10.4314/rjeste.v3i1.6s

De Boer, J., Wouter Botzen, W. J., & Terpstra, T. (2015). More than fear induction: Toward an understanding of people's motivation to be well-prepared for emergencies in flood-prone areas. *Risk analysis*, 35(3), 518-535. https://doi.org/10.1111/risa.12289

Dube, K., Nhamo, G., & Chikodzi, D. (2022). Flooding trends and their impacts on coastal communities of Western Cape Province, South Africa. *GeoJournal*, 87(S4), 453–468. https://doi.org/10.1007/s10708-021-10460-z

Bubeck, P., Botzen, W. J. W., Suu, L. T. T., & Aerts, J. C. J. H. (2012). Do flood risk perceptions provide useful insights for flood risk management? Findings from central Vietnam. *Journal of Flood Risk Management*, *5*(4), 295–302. https://doi.org/10.1111/j.1753-318X.2012.01151.x

Cai, S., Fan, J., & Yang, W. (2021). Flooding risk assessment and analysis based on GIS and the TFN-AHP method: A case study of Chongqing, China. *Atmosphere*, *12*(5). https://doi.org/10.3390/atmos12050623

Cirella, G. T., Iyalomhe, F. O., & Cirella, G. T. (2018). Flooding in Benin City, Nigeria. CONFERENCE *Proceedings of the 2nd International Conference on Sustainability, Human Geography and Environment,* Kraków · Poland, 175-179.

Collentine, D., & Futter, M. N. (2018). Realising the potential of natural water retention measures in catchment flood management: trade-offs and matching interests. *Journal of Flood Risk Management*, 11(1), 76–84. https://doi.org/10.1111/jfr3.12269

Cutter, S. L., Barnes, L., Berry, M., Burton, C., Evans, E., Tate, E., & Webb, J. (2008). A place-based model for understanding community resilience to natural disasters. *Global Environmental Change*, *18*(4), 598–606. https://doi.org/10.1016/j.gloenvcha.2008.07.013

Estrada, F., Perron, P., & Yamamoto, Y. (2023a). Anthropogenic influence on extremes and risk hotspots. *Scientific Reports*, *13*(1). https://doi.org/10.1038/s41598-022-27220-9

Gamoyo, M., Reason, C., & Obura, D. (2015). Rainfall variability over the East African coast. *Theoretical and Applied Climatology*, *120*(1–2), 311–322. https://doi.org/10.1007/s00704-014-1171-6

Gerard, H. (2014). Design of Appropriate hydraulic structures for sustainable flood control in the Nyabugogo catchment, with focus on the Mpazi sub catchment [Doctoral dissertation*,* University of Rwanda].

Google Earth Pro. (2023). *Google Earth Pro*. Retrieved October 11, 2023, https://www.google.com/intl/tr/earth/about/

Habonimana, H. V., Bizimana, J. P., Uwayezu, E., Tuyishimire, J., & Mugisha, J. (2015, November 18-20). Integrated flood modelling *for flood hazard assessment in Kigali city, Rwanda* [Conference presentation]. GeoTechRwanda, Kigali, Ruanda.

Hadipour, V., Vafaie, F., & Deilami, K. (2020). Coastal flooding risk assessment using a GIS-based spatial multi-criteria decision analysis approach. *Water 12*(9). https://doi.org/10.3390/W12092379

Holstead, K. L., Kenyon, W., Rouillard, J. J., Hopkins, J., & Galán-Díaz, C. (2017). Natural flood management from the farmer's perspective: criteria that affect uptake. *Journal of Flood Risk Management*, 10(2), 205–218. https://doi.org/10.1111/jfr3.12129

Hu, S., Cheng, X., Zhou, D., & Zhang, H. (2017). GIS-based flood risk assessment in suburban areas: A case study of the Fangshan district, Beijing. *Natural Hazards*, 87(3), 1525–1543. https://doi.org/10.1007/s11069-017-2828-0

Khedo, K. K. (2013). Real-time flood monitoring using wireless sensor networks. *The Journal of the Institution of Engineers Mauritius-IEM Journal,* 1, 59-69.

Loke, A. Y., Guo, C., & Molassiotis, A. (2021). Development of disaster nursing education and training programs in the past 20 years (2000–2019): A systematic review. *Nurse Education Today*, *99*. https://doi.org/10.1016/j.nedt.2021.104809

Manyifika, M. (2015). Diagnostic assessment on urban floods using satellite data and hydrologic models in Kigali, Rwanda [Master's thesis, University of Twente]. Faculty of Geo-Information Science and Earth Observation. https://essay.utwente.nl/84041/1/manyifika.pdf

Mashi, S. A., Inkani, A. I., Obaro, O., & Asanarimam, A. S. (2020). Community perception, response and adaptation strategies towards flood risk in a traditional African city. *Natural Hazards*, *103*(2), 1727–1759. https://doi.org/10.1007/s11069-020-04052-2

Mind'je, R., Li, L., Amanambu, A. C., Nahayo, L., Nsengiyumva, J. B., Gasirabo, A., & Mindje, M. (2019). Flood susceptibility modelling and hazard perception in Rwanda. *International Journal of Disaster Risk Reduction*, *38*. https://doi.org/10.1016/j.ijdrr.2019.101211

Mohammadreza Hassani, E., Vessalas, K., Sirivivatnanon, V., & Baweja, D. (2017). Influence of permeability-reducing admixtures on water penetration in concrete. *ACI Materials Journal*, *114*(6), 911–922. https://doi.org/10.14359/51701002

Njogu, H. W. (2021). Effects of floods on infrastructure users in Kenya. *Journal of Flood Risk Management*, 14(4). https://doi.org/10.1111/jfr3.12746

Pant, R., Thacker, S., Hall, J. W., Alderson, D., & Barr, S. (2018). Critical infrastructure impact assessment due to flood exposure. *Journal of Flood Risk Management*, *11*(1), 22–33. https://doi.org/10.1111/jfr3.12288

Peker, İ. B., Gülbaz, S., Demir, V., Orhan, O., & Beden, N. (2024). Integration of HEC-RAS and HEC-HMS with GIS in flood modeling and flood hazard mapping. *Sustainability,* *16*(3). https://doi.org/10.3390/su16031226

Pörtner, H. O., Roberts, D. C., Masson-Delmotte, V., Zhai, P., Tignor, M., Poloczanska, E., & Weyer, N. M. (2019). The ocean and cryosphere in a changing climate. *IPCC special report on the ocean and cryosphere in a changing climate, 1155*.

Poussin, J. K., Wouter Botzen, W. J., & Aerts, J. C. J. H. (2015). Effectiveness of flood damage mitigation measures: Empirical evidence from French flood disasters. *Global Environmental Change*, *31*, 74–84. https://doi.org/10.1016/j.gloenvcha.2014.12.007

Ribas, A., Olcina, J., & Sauri, D. (2020). More exposed but also more vulnerable? Climate change, high intensity precipitation events and flooding in Mediterranean Spain. *Disaster Prevention and Management*, 29(3), 229–248. https://doi.org/10.1108/DPM-05-2019-0149

Rimba, A., Setiawati, M., Sambah, A., & Miura, F. (2017). Physical flood vulnerability mapping applying geospatial techniques in Okazaki city, Aichi prefecture, Japan. *Urban Science*, *1*(1), 7. https://doi.org/10.3390/urbansci1010007

Roy, D. C., & Blaschke, T. (2015). Spatial vulnerability assessment of floods in the coastal regions of Bangladesh. *Geomatics, Natural Hazards and Risk*, 6(1), 21–44. https://doi.org/10.1080/19475705.2013.816785

Saaty, T. L. (2002). Decision making with the Analytic Hierarchy Process. *Scientia Iranica*, 9(3), 215–229. https://doi.org/10.1504/ijssci.2008.017590

Seddon, N., Chausson, A., Berry, P., Girardin, C. A. J., Smith, A., & Turner, B. (2020). Understanding the value and limits of nature-based solutions to climate change and other global challenges. *Philosophical Transactions of the Royal Society B: Biological Sciences*, 375(1794). https://doi.org/10.1098/rstb.2019.0120

Shivaprasad Sharma, S. V., Roy, P. S., Chakravarthi, V., & Srinivasa Rao, G. (2018). Flood risk assessment using multi-criteria analysis: A case study from Kopili river basin, Assam, India. *Geomatics, Natural Hazards and Risk*, *9*(1), 79–93. https://doi.org/10.1080/19475705.2017.1408705

Taramelli, A., Lissoni, M., Piedelobo, L., Schiavon, E., Valentini, E., Xuan, A. N., & Gonz, D. (2019). Monitoring green infrastructure for natural water retention using Copernicus global land products. *Remote Sensing,* 11(13), 1583. https://doi.org/10.3390/rs11131583

UNICEF. (2018). *UNICEF annual report 2017: for every child, results*. UNICEF. Retrieved October 11, 2023, https://www.unicef.org/reports/unicef-annual-report-2017

Wahab, B., & Falola, O. (2022). Vulnerable households in flood-prone communıtıes in Ibadan: Measures to improve theır status wıthın the inclusıve Ibadan city framework. *Journal of Inclusive Cities and Built Environment*, 21–27. https://doi.org/10.54030/2788-564x/2022/cp1v2a6

Wali, U. G., Munyaneza, O., Nzeyimana, Y. K., & Wali, U. G. (2013). Hydraulic structures design for flood control in the Nyabugogo Wetland, Rwanda. *Nile Basin Water Science & Engineering Journal*, 6(2), 26-37.

Wang, W., Shao, Q., Yang, T., Peng, S., Xing, W., Sun, F., & Luo, Y. (2013). Quantitative assessment of the impact of climate variability and human activities on runoff changes: A case study in four catchments of the Haihe River basin, China. *Hydrological Processes*, *27*(8), 1158–1174. https://doi.org/10.1002/hyp.9299

Wilkinson, M. E., Addy, S., Quinn, P. F., & Stutter, M. (2019). Natural flood management : small-scale progress and larger-scale challenges. *Scottish Geographical Journal,* 135(1-2), 23-32. https://doi.org/10.1080/14702541.2019.1610571

Zeleňáková, M., Vido, J., Portela, M. M., Purcz, P., Blištán, P., Hlavatá, H., & Hluštík, P. (2017). Precipitation trends over Slovakia in the period 1981-2013. *Water*, *9*(12), 922. https://doi.org/10.3390/w9120922